The Abdus Salam
International Centre for Theoretical Physics

United Nations
Educational, Scientific and
Cultural Organization

IAEA
International Atomic Energy Agency

1856-67

2007 Summer College on Plasma Physics

30 July - 24 August, 2007

Nonlinear mirror mode dynamics

E. Kuznetsov
Landau Institute of Theoretical Physics and P. N. Lebedev Physical Institutut, Moscow

Nonlinear mirror mode dynamics:
simulations and modeling

P.L. Sulem, T. Passot, D. Borgogno
CNRS, Observatoire de la Côte d'Azur, Nice

E. Kuznetsov
Landau Institute of Theoretical Physics and
P. N. Lebedev Physical Institutut, Moscow

F. Califano
Dipartimento di Fisica, Universita' di Pisa

P. Hellinger, P. Travnicek
Institute of Atmospheric Physics, Prague

ICTP, Trieste, August 2007

Outline

1. Satellite observations
2. Vlasov simulations
3. Theoretical interpretation
4. Mechanisms of hole formation
5. Fluid model for mirror modes
6. Conclusions
7. Open questions

1. Satellite observations

Quasi-stationary magnetic structures in the plasma frame (**holes or humps**), are commonly observed in the solar wind and the planetary magnetosheaths.

A: Peaks in low field regions

B: Dips in high field regions

C: Nearly sinusoidal

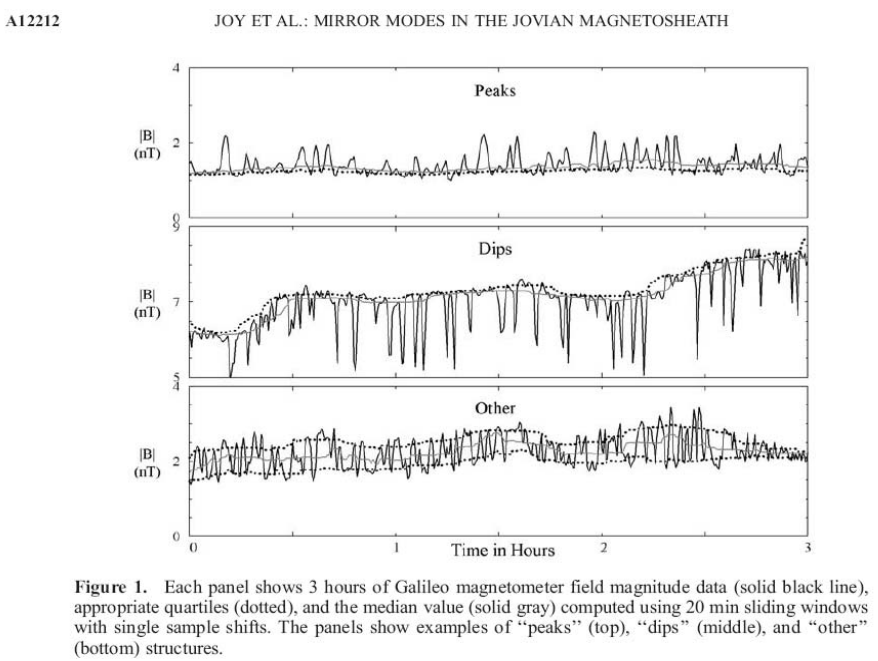

Figure 1. Each panel shows 3 hours of Galileo magnetometer field magnitude data (solid black line), appropriate quartiles (dotted), and the median value (solid gray) computed using 20 min sliding windows with single sample shifts. The panels show examples of "peaks" (top), "dips" (middle), and "other" (bottom) structures.

Joy et al. J. Geophys. Res. **111**, A12212 (2006)

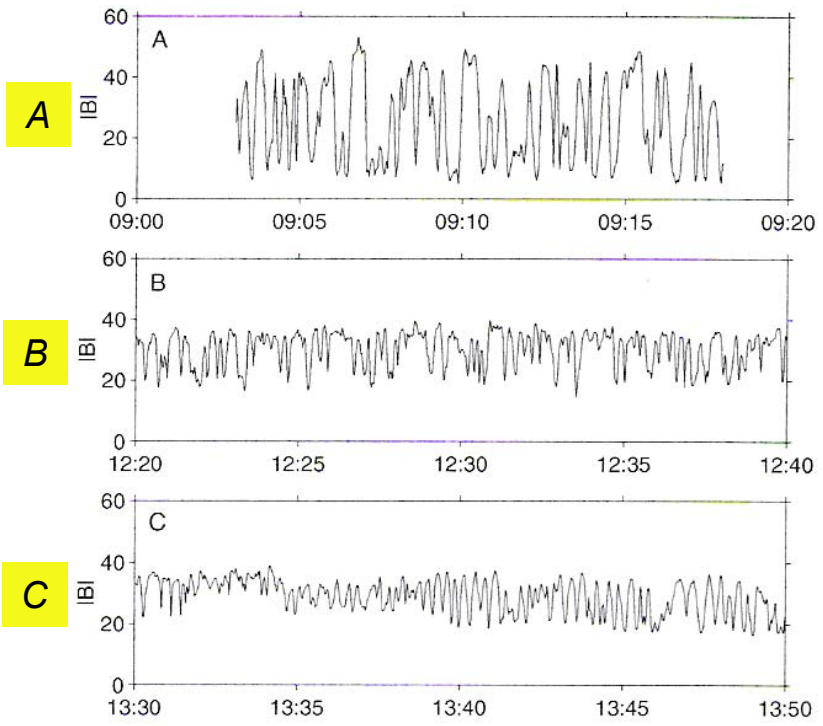

Figure 2. A, B and C show the field magnitude recorded during three intervals from 20 Dec 1997. They illustrate three forms of mirror structure: peaks, dips and a near sinusoidal waveform.

Structures observed in the magnetosheath

Lucek et al. GRL **26,** 2159 (1999)

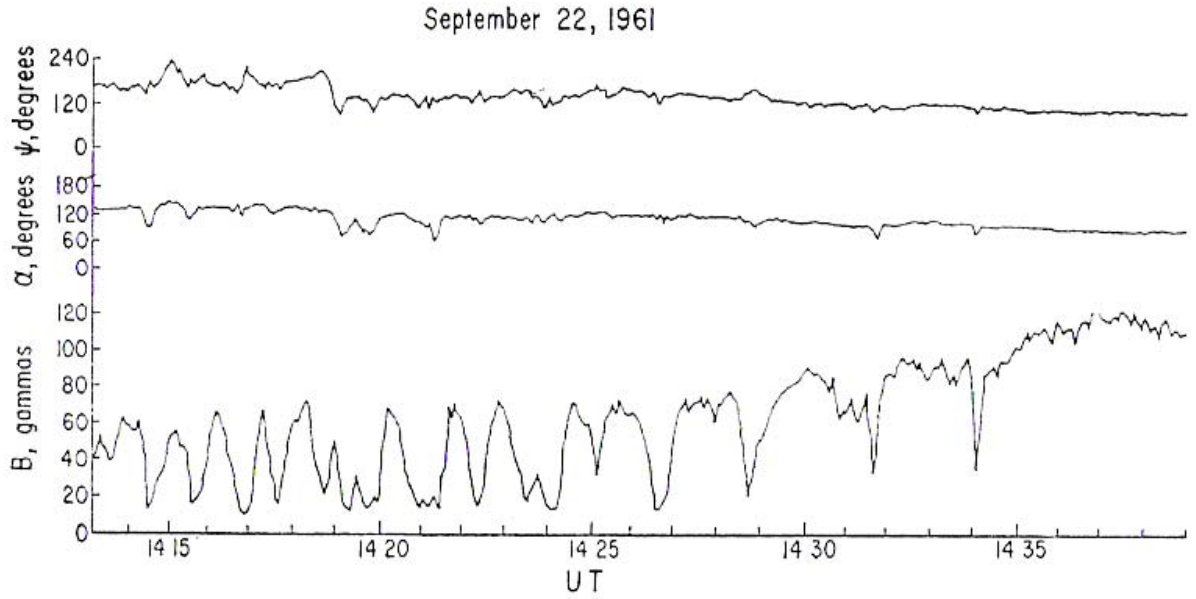

Fig. 1. Magnetic field magnitude B and direction angles α and ψ are presented in satellite coordinates for part of a highly disturbed orbit. The angle between the magnetic field and the satellite spin axis is α. The angle between the magnetic field and the sun, as projected onto the satellite's equatorial plane is ψ. Each point plotted represents the average of 16 individual field measurements taken during a 5-sec time interval.

Kaufmann et al., J. Geophys. Res. **75,** 4666 (1970)

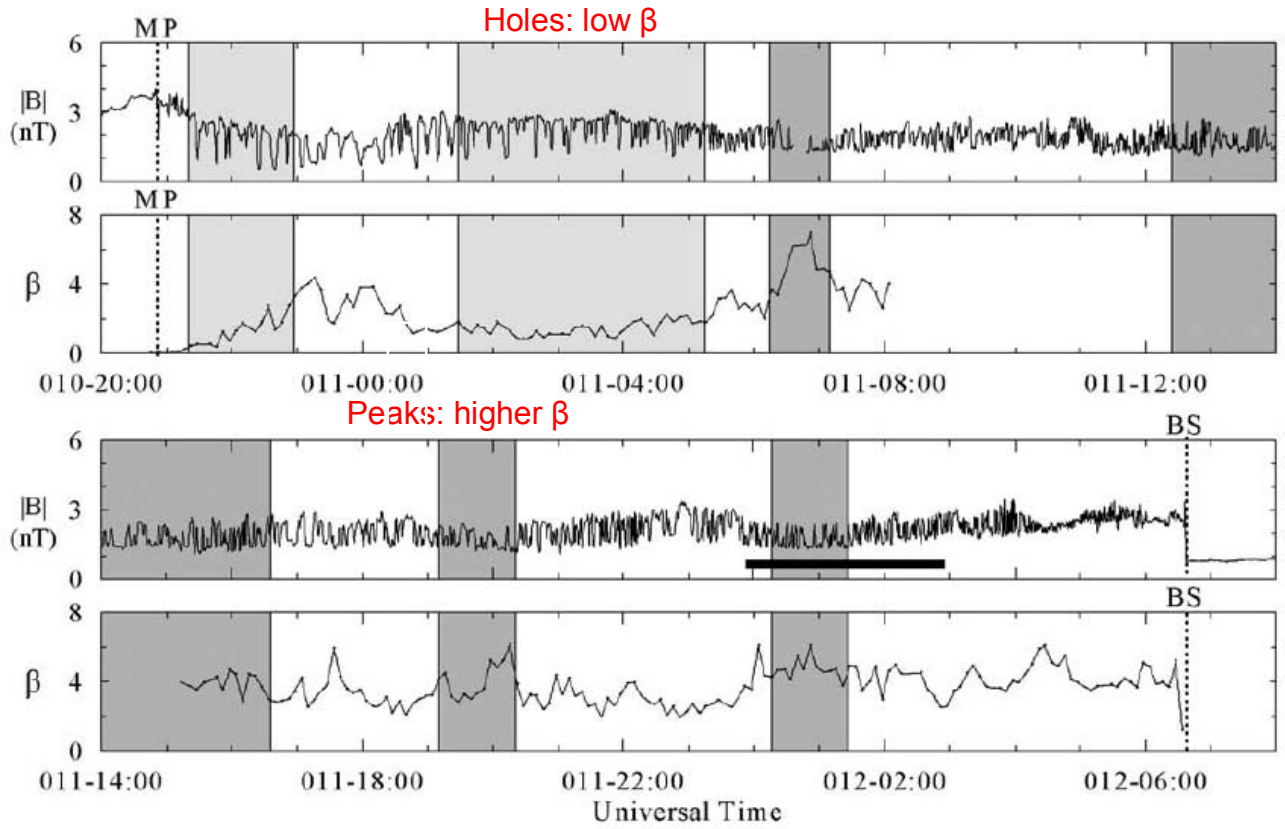

Figure 8. Galileo magnetic field and plasma β observations from the outbound pass of the 29th orbit. The shading convention used here is the same as in Figure 2. The heavy black line indicates an interval of amplitude saturation. The vertical dotted lines mark the bow shock and magnetopause crossing times.

Depending on local values of β, magnetic holes or humps are preferentially formed.

Same conclusion by Bavassano-Cattaneo et al. 1998 (Saturn's magnetosheath) ,
Soucek, Lucek & Dandouras 2007 (Earth's magnetosheath).

Stability properties amenable to a simple energetic argument in the framework of anisotropic MHD with (quasi-isothermal) equations of state appropriate for slow dynamics

(Passot, Ruban & Sulem, PoP, 13, 102310, 2006)

Free solar wind
(Ulysses)

Jovian magnetosheath
(Ulysses)

Free solar wind
(Helios)

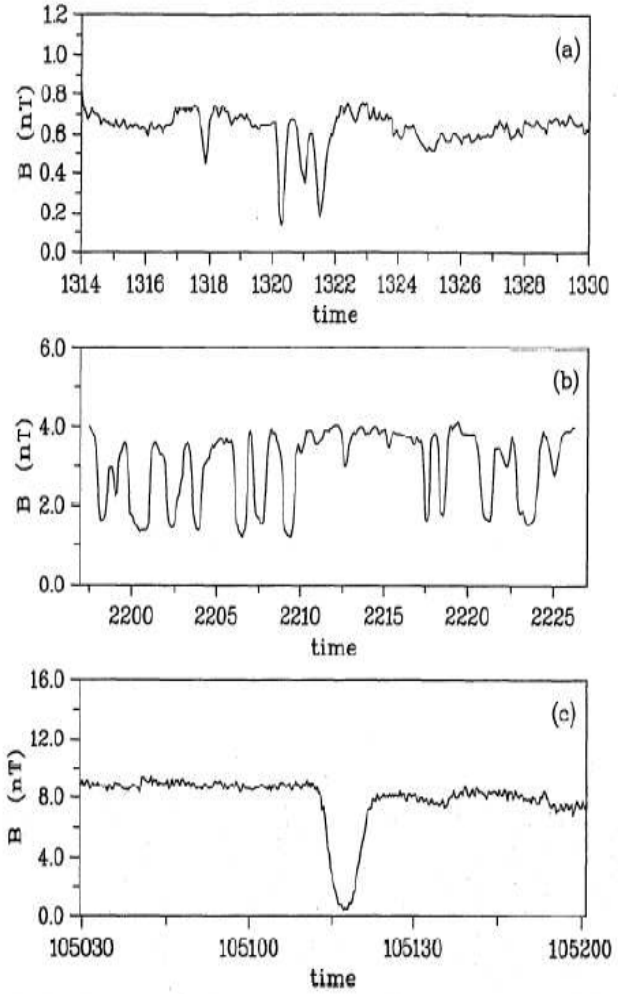

Figure 1. Examples of magnetic holes observed (a) by Ulysses in the free solar wind (taken from Figure 2 of *Winterhalter et al.* [1994], (b) by Ulysses in the magnetosheath of Jupiter, called mirror mode structures (from Figure 5 of *Erdös and Balogh* [1996]), and (c) by Helios in the free solar wind (data courtesy of K. Sperveslage and F.M. Neubauer, University of Köln, 1999). Shown is the magnetic field magnitude.

Magnetic holes may display different shapes (sharp or roundish). Do they have a unique origin?

Baumgärtel JGR **104** (A12), 28295 (1999)

Main properties:

- Structures are quasi-static in the plasma frame,
- Observed in regions displaying: ion temperature anisotropy $T_{i\perp} > T_{i\parallel}$
  β of a few units

(conditions met under the effect of plasma compression in front of the magnetopause).

- Mostly longitudinal magnetic field fluctuations.
- Density is anticorrelated with magnetic field amplitude.
- Size of these structures: a few Larmor radii.
- 3D shape is cigar-like, quasi-parallel to the ambient field.

Origin of these structures is still not fully understood.
Usually viewed as nonlinearly saturated states of the mirror instability.

Other recent interpretations:

- trains of slow-mode magnetosonic solitons (Stasiewicz 2004)
- mirror instability is the trigger, generating high amplitude fluctuations that evolve such as to become nonlinear solutions of isotropic or anisotropic plasma equations (Baumgärtel, Sauer & Dubinin 2005)

Mirror instability:

Extensively studied in the linear regime:

Venedov and Sagdeev (1958), Hasegawa (1969), Hall (1979)
Gary (1992), McKean et al. (1992,1994), Southwood and Kivelson (1993),
Pokhotelov et al. (2004 and references therein), Hellinger (2007).

- Requires ion temperature anisotropy ($T_{i\perp} > T_{i\parallel}$) and sufficiently large β.

- Zero-frequency instability.

- At least near threshold, develops at large angle with respect to ambient magnetic field.

  (At small or moderate angle and/or smaller β, Ion Cyclotron Anisotropic instability can be dominant).

- Driven by Landau wave-particle resonance and quenched at small-scales (usually at a fraction of the ion Larmor radius) by finite Larmor radius effects.

Theory of the nonlinear regime still incomplete.

Magnetic holes are also observed in conditions for which the plasma is linearly stable (BISTABILITY).

$$\frac{T_\perp}{T_\parallel} - 1 > \frac{1}{\beta_\perp}$$

(instability condition for bi-Maxwellian distribution)

Skewness of magnetic fluctuations:
- when negative: magnetic holes
- when positive: magnetic humps

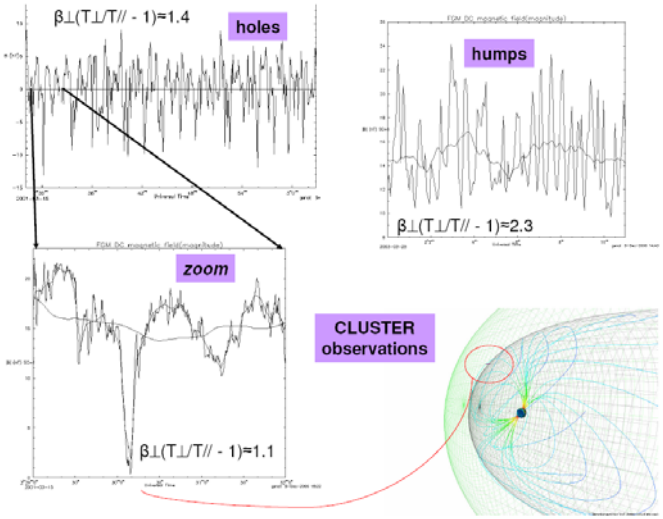

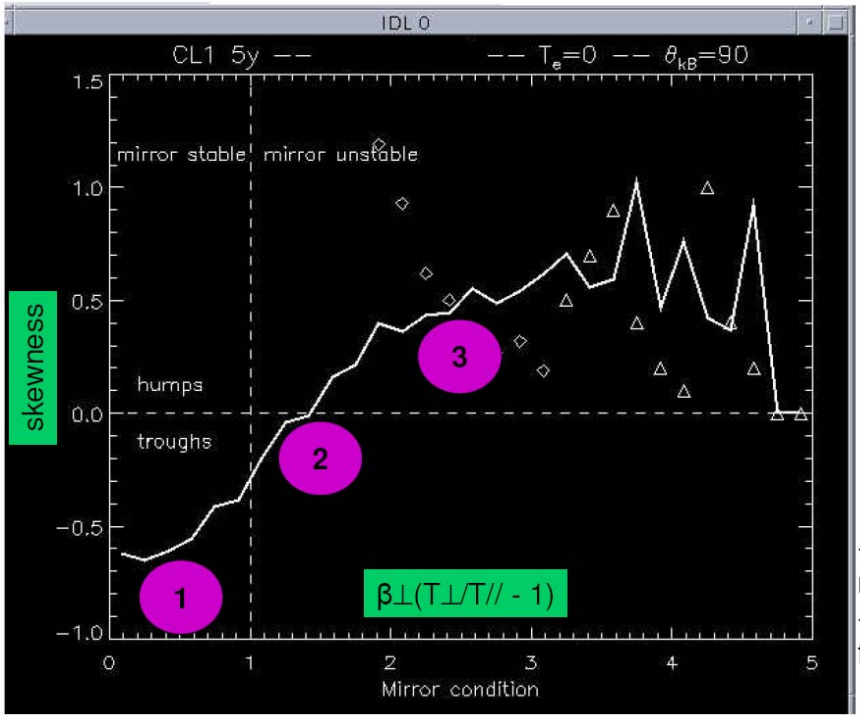

Distance to threshold

1
- Holes in small beta region
-Linearly stable or close to threshold
- *Bistability* region

2
- Linear mirror mode
- Classical sinusoidal shape

3
- Humps in large or moderate beta region
- Corresponds to the first phase of simulations

Magnetosheath CLUSTER data (Génot et al., AGU 2006)

Soucek, Lucek & Dandouras 2007: "peaks are typically observed in an unstable plasma, while mirror structures observed deep within the stable region appear almost exclusively as dips."

Bistability also observed in Jovian magnetosheath (Erdös and Balogh 1996)

Observational data thus suggest that for fixed $T_\perp / T_\parallel$,magnetic holes are obtained for relatively small β and magnetic humps for relatively large β.

This effect can be understood on the basis of an energetic argument in the context of usual anisotropic MHD with a suitable equations of state

$$\frac{T_\parallel}{T_\parallel^{(0)}} = 1 \quad ; \quad \frac{T_\perp}{T_\perp^{(0)}} = \frac{B/B_0}{(A+1)B/B_0 - A}, \qquad (A = \frac{T_\perp^{(0)}}{T_\parallel^{(0)}} - 1)$$

obtained by closing the STATIONARY fluid hierarchy, assuming a bi-Maxwellian distribution function.

The problem of stationary structures is amenable of a variational formulation.

On stationary configurations, the functional

$$\mathcal{H} = \int \left(\frac{\overline{B}^2}{\beta_\parallel} + n \left[F(\overline{B}) + \ln n - 1 \right] + 1 \right) d\mathbf{r}$$

(where $F(\overline{B}) = \ln[(A+1)\overline{B} - A] - \ln \overline{B}$. and $\overline{B} = B/B^{(0)}$) should achieve a minimal value.

This model that does not include kinetic effects could possibly be relevant to describe the very large magnetic holes (hundreds to thousands of ion Larmor radii), observed in the solar wind (Stephen and Kasper, JGR 2007).

Passot, Ruban, Sulem, PoP **13**, 102310 (2006)

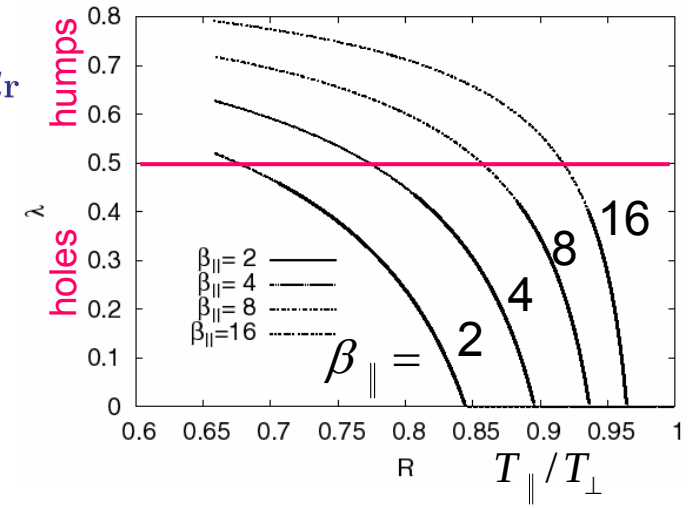

thick lines : bistability

2. Direct numerical simulations of the Vlasov-Maxwell equations

Shed light on the time evolution and the origin of the structures.

Mirror unstable regime relatively near threshold in a large domain

With a PIC code in a large domain:
1024 cells with 500 000 particles/cell;
Domain size= 2048 c/ω_{pi}
Growth rate: 0.005 Ω_p^{-1}

$\theta_{kB} = 72.8°$ (most unstable direction)
$\beta_{p\parallel} = 1 \; \beta_{p\perp} = 1.857 \quad \beta_e = 10^{-2}$

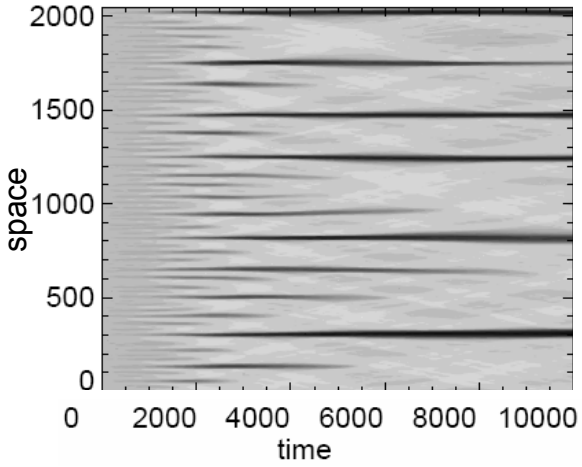

Gray scale plot of the magnetic field fluctuations perpendicular to the direction of variation, as a function of space and time.

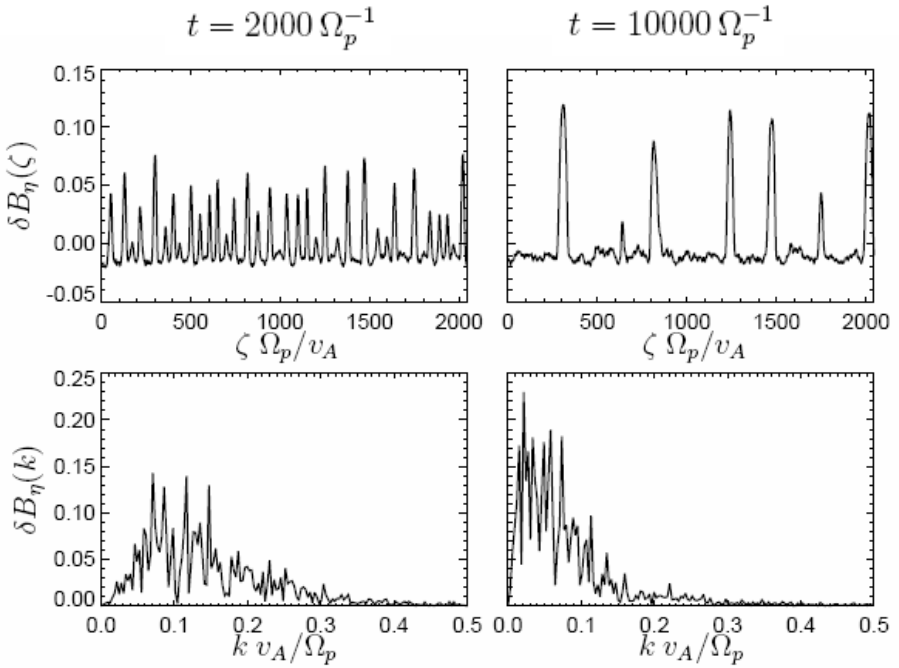

A large number of modes are excited
Humps form and undergo coarsening.

Linear phase

magnetic humps

magnetic holes

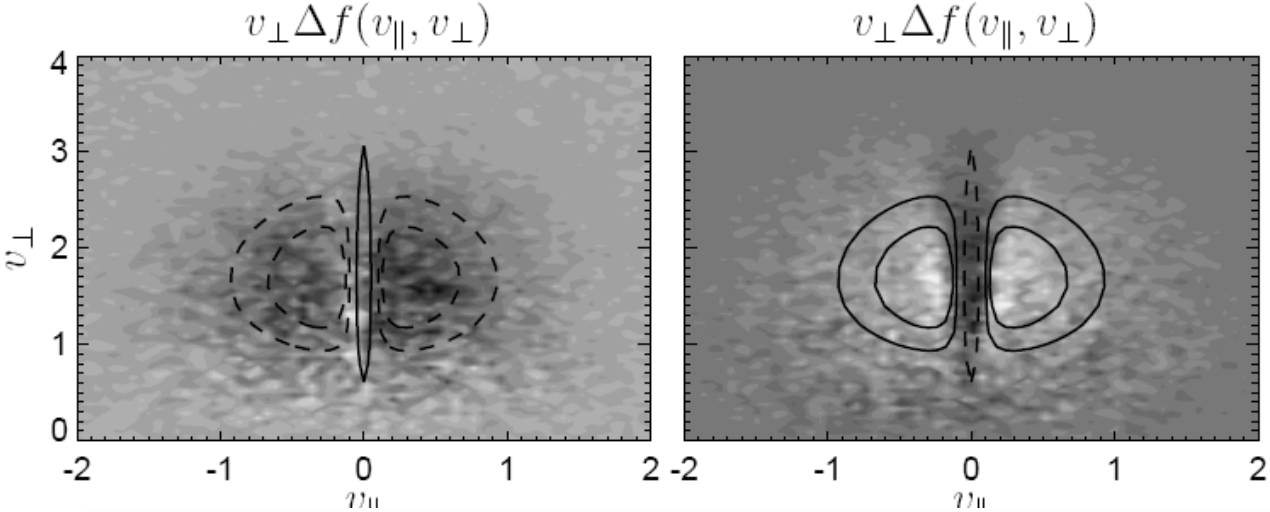

The more noisy aspect of the distribution perturbation in the magnetic humps is due to the poorer statistics in these regions.

Figure 2. Changes in the distribution function at the time $t = 1000/\Omega_p$ in regions with $\delta B_\eta/B_0 > 0.01$ (left) and $\delta B_\eta/B_0 < -0.01$ (right). The overplotted curves show the theoretical linear response $v_\perp \delta f$ corresponding to the most unstable mode at maximum δB_η (left) and minimum δB_η (right): solid and dashed curves denotes positive and negative values of $v_\perp \delta f$, respectively.

$$\delta f = \frac{q}{m}\left(\frac{k_\parallel v_\perp}{k_\parallel v_\parallel - \omega}\frac{\partial f_0}{\partial v_\parallel} - \frac{\partial f_0}{\partial v_\perp}\right)\frac{\delta B_\parallel}{B_0}$$

time $t = 1000/\Omega_p$: approximatively the end of the linear phase.

MAIN QUESTION: processes leading to the saturation of the linear instability.

Mechanism first suggested: based on quasi-linear theory (Shapiro and Shevshenko 1963)

- Assumes space homogeneity (thus absence of coherent structures)
- Can thus be valid at early times only
- Requires many modes in interaction: extended domain
- Mainly associated with a diffusion process in velocity space, dominantly along the ambient field.

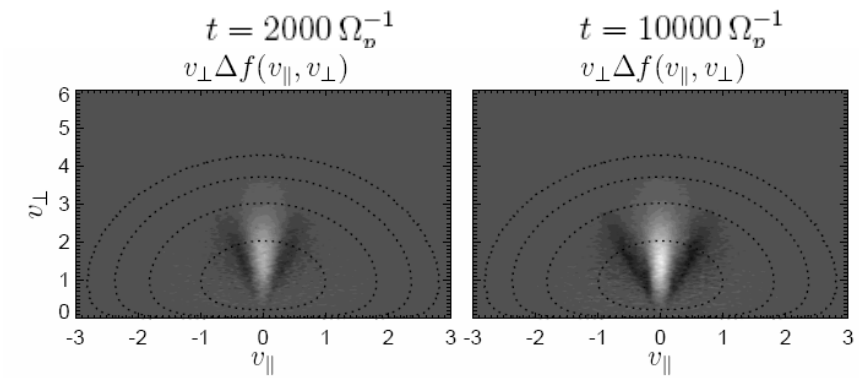

$\Delta f(v_\parallel, v_\perp)$ corresponds to the variation of the space averaged distribution function from the initial to the considered time. In the white regions, (whose localization corresponds to small parallel velocities), the distribution function is reduced, while in adjacent black regions, it is increased.

Dotted lines : contours of the initial equilibrium distribution function.

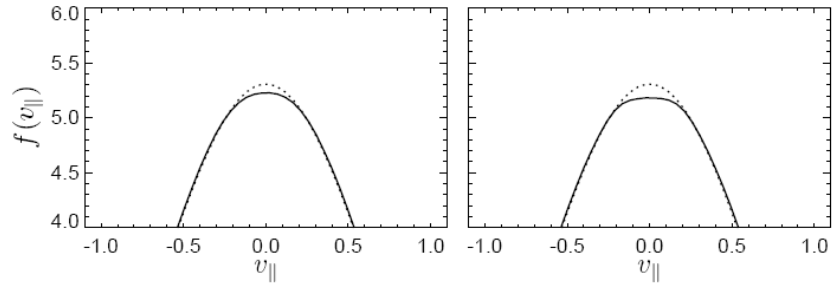

Reduced distribution function f as a function of $v_\parallel$ (solid curve) compared to the initial reduced distribution function (dotted curve).

Flattening of the distribution function resulting from the diffusion in velocity space.

Space averaging is needed to make quasi-linear theory conspicuous

(it eliminates the contribution of the linear response function that is pointwise dominant).

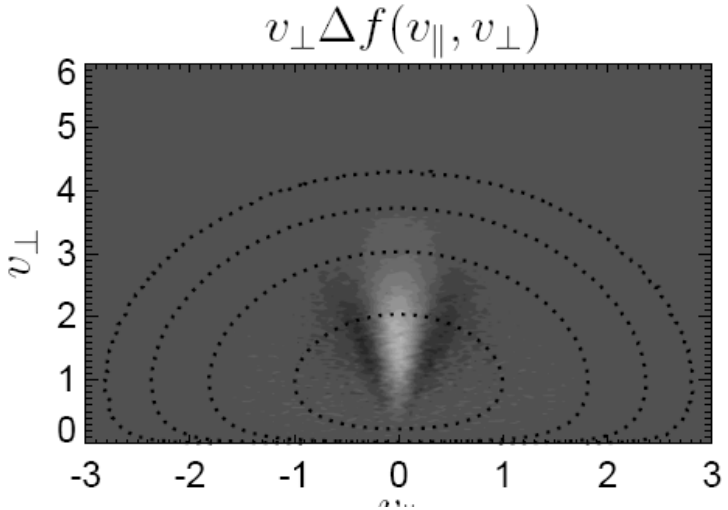

simulation

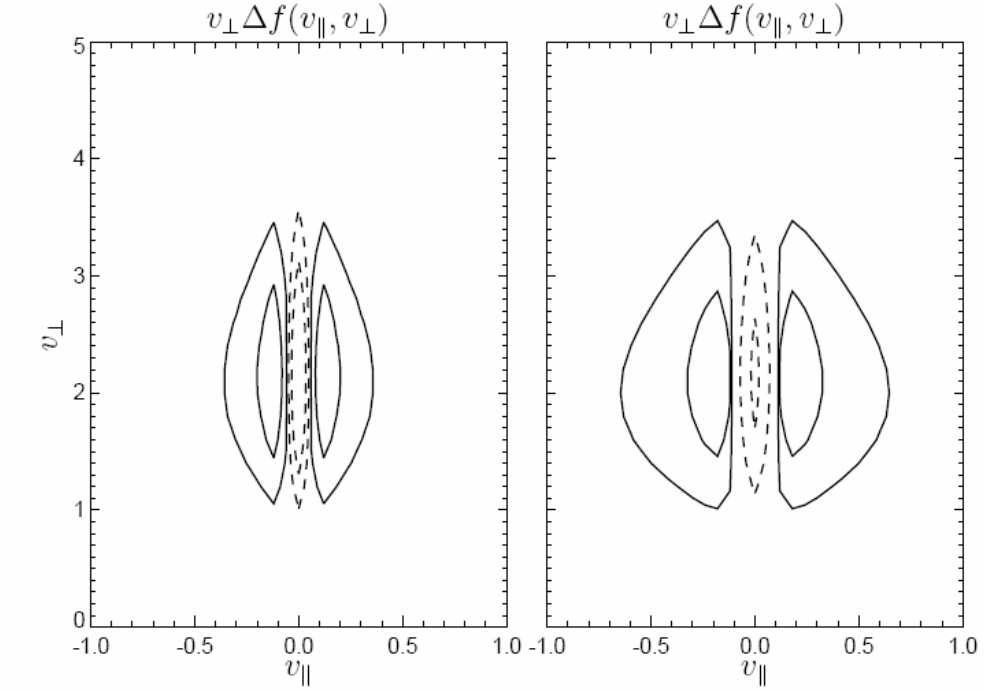

Figure 4. Schematic view of the prediction of the quasilinear theory: Effect of the quasilinear diffusion Δf on the distribution function, a contribution of (left) the most unstable mode and of (right) a weakly unstable mode. Solid (dashed) contours show positive (negative) values.

Fluctuating magnetic energy

Gray scale plot of the magnetic fluctuations as a function of space and time.

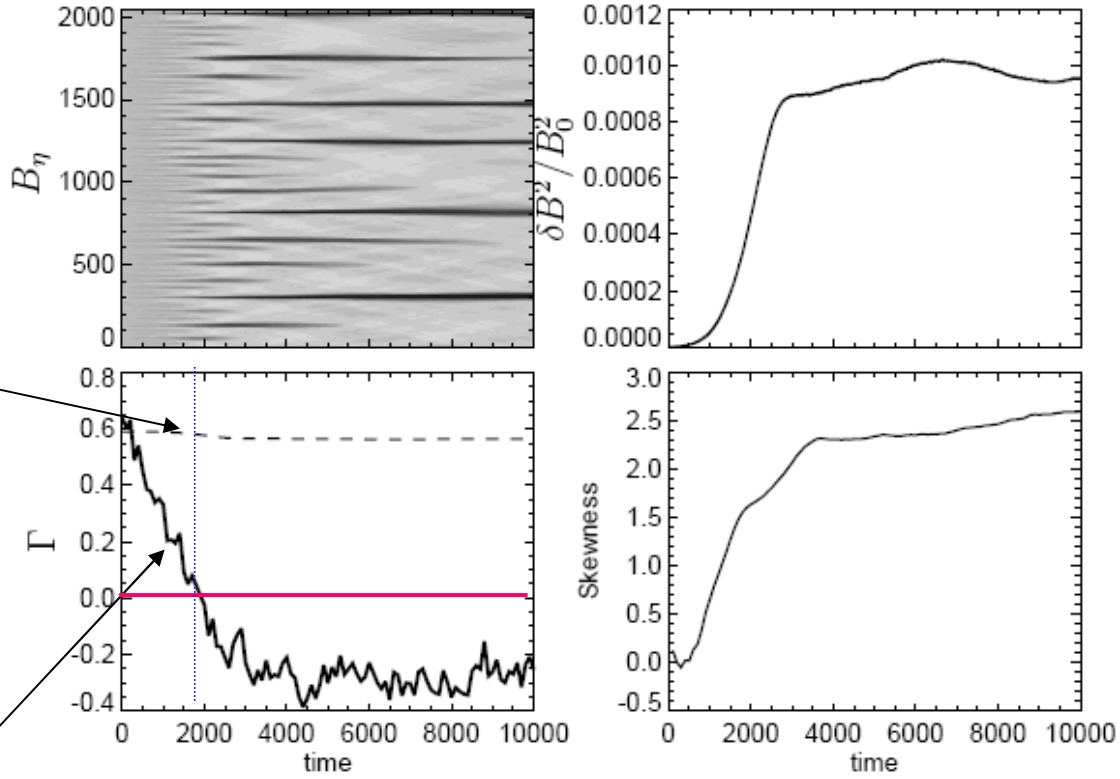

Bi-Maxwellian distance to threshold:

$$\Gamma^* = \beta_\perp \left(\frac{T_\perp}{T_\parallel} - 1 \right) - 1$$

Instantaneous distance to threshold:

$$\Gamma = -\frac{m}{p_B} \int \frac{v_\perp^4}{4} \frac{\partial f}{\partial v_\parallel^2} d^3v - \beta_\perp - 1$$

Distance to threshold reaches negative values, a signature that quasi-linear theory ceases to apply when coherent structures begin to form.

The instability continues to take place due to hydrodynamic-type nonlinearity.

Positive skewness: magnetic humps.

Hybrid simulations at moderate β (Baumgärtel, Sauer & Dubinin, GRL, 2003)

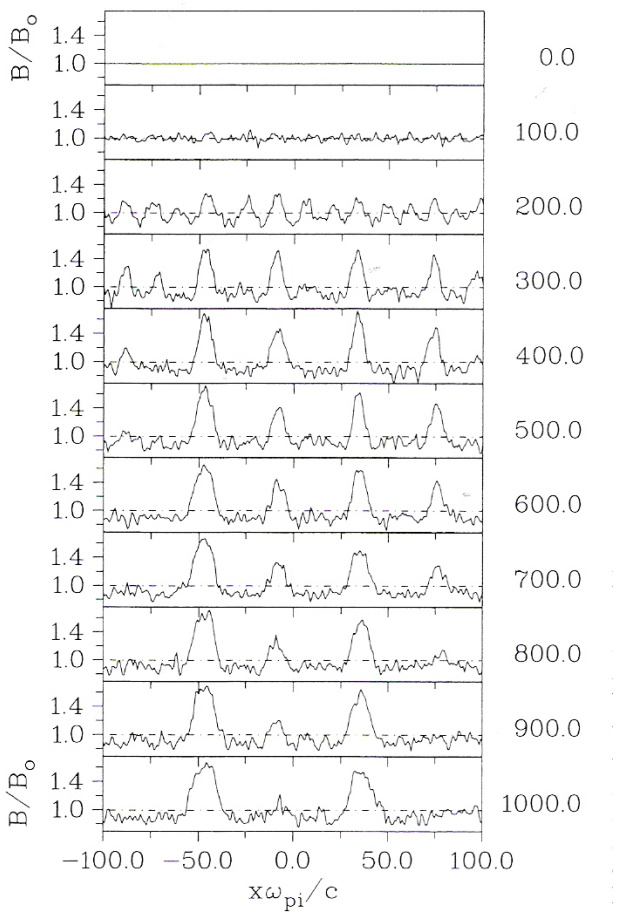

Figure 4. Space-time evolution of the magnetic field in an uniform, collisionless, anisotropic, mirror-unstable plasma with bi-Maxwellian proton distribution ($\beta_{i\perp} = 5$, $\beta_{i\parallel} = 2.5$, $\beta_e = 1$, $\theta = 80°$.

Initial random noise in a mirror instable regime leads to the formation of magnetic humps whose number decreases as time elapses.

A localized magnetic perturbation in the form of a finite amplitude hump relaxes

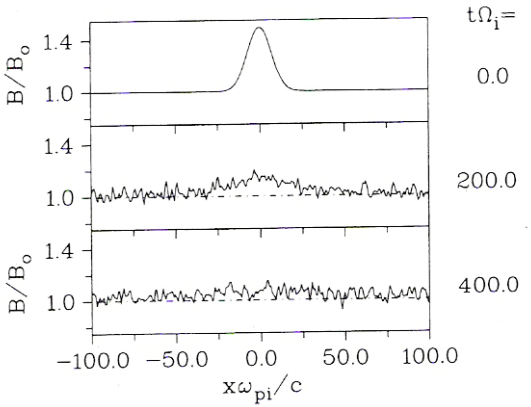

Figure 3. Space-time evolution of a magnetic compression $\delta B_z/B_0 = 0.5 \exp(-x^2/h^2)$, other parameters the same as in Figure 1.

A localized magnetic perturbation in the form of a finite-amplitude hole persists

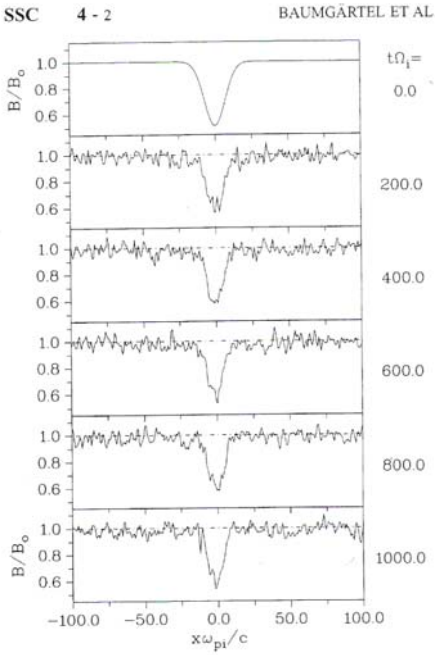

Figure 1. Space-time evolution of a magnetic depression in an otherwise uniform, collisionless, isotropic high-β plasma with $\beta_i = 2.5$, $\beta_e = 1$, $\theta = 80°$. The initial perturbation is prescribed as $\delta B_z/B_0 = -0.5 \exp(-x^2/h^2)$ with $h = 10\ c/\omega_{pi}$; δB_y is set to zero at $t = 0$.

In a small domain, the quasi-linear phase is not present

With an Eulerian code, in a small domain (15x $2\pi\ c/\omega_{pi}$),

$\beta_{\parallel}=15$, $T_{\perp}/T_{\parallel}=1.4$ and $\theta=1.37$

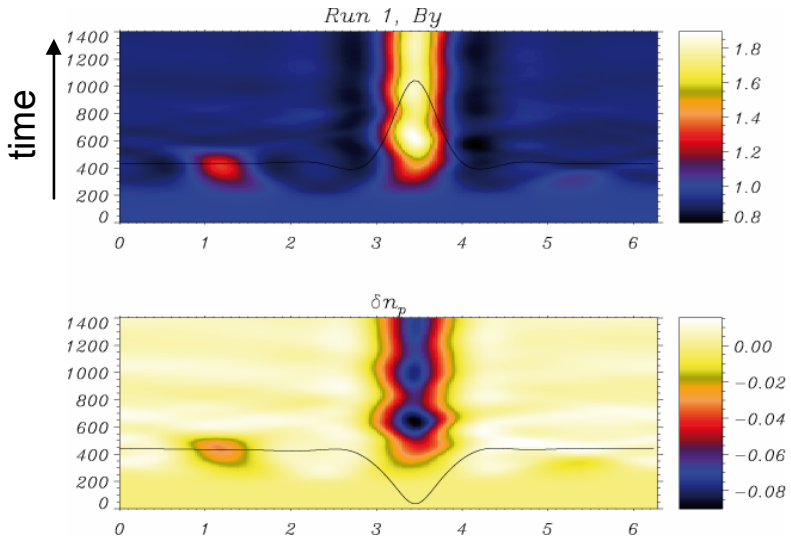

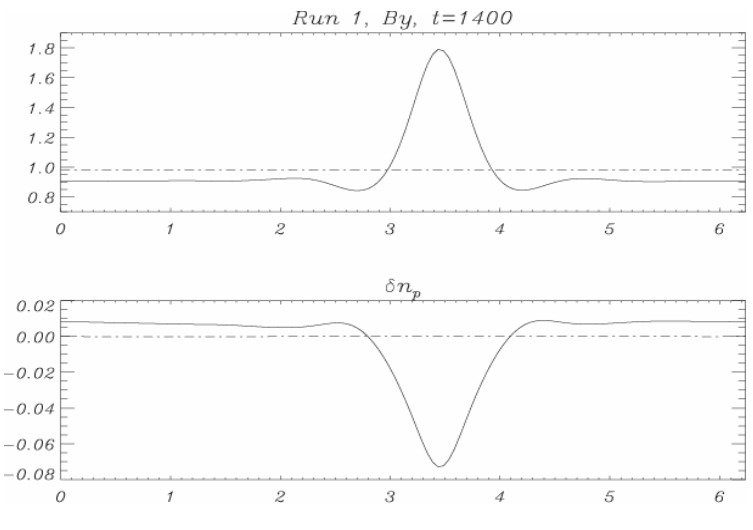

Magnetic hump (and density hole) resulting from the mirror instability, starting from noise.

Magnetic humps form even very close to threshold

$$\beta_{\|} = 6, \quad \theta = 1.463, \quad T_{\perp}/T_{\|} = 1.25$$

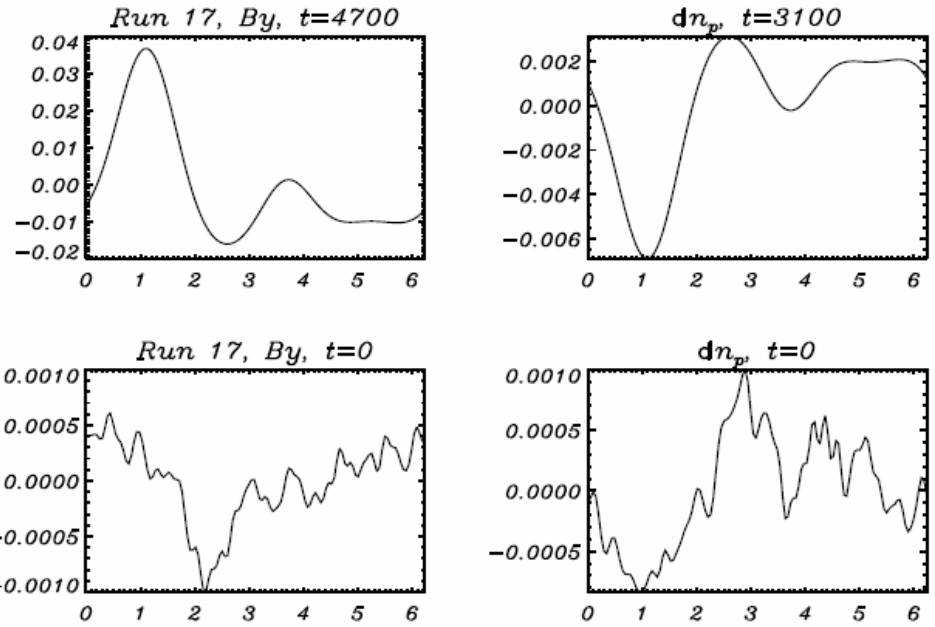

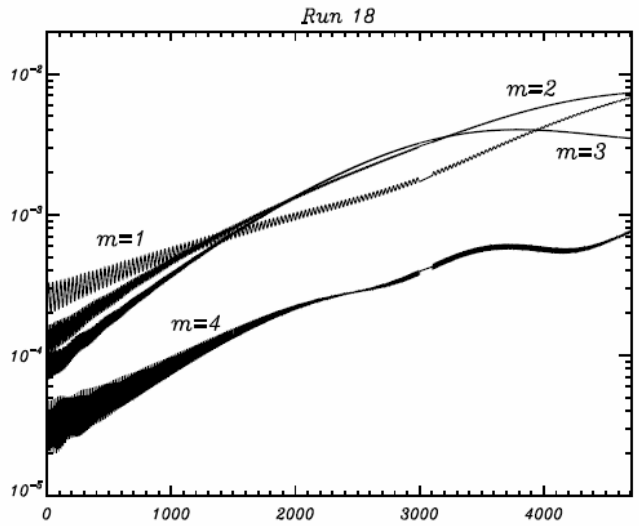

Time evolution of the unstable modes

Growth rate of most unstable mode (m=3) : 0.0017 Ωi

Distribution function does not display flattening (in contrast with simulations in large boxes):
No quasi-linear phase.

High resolution in velocity space nevertheless required.

Structure formation: amenable to a **reductive perturbative expansion** of the Vlasov-Maxwell equations.

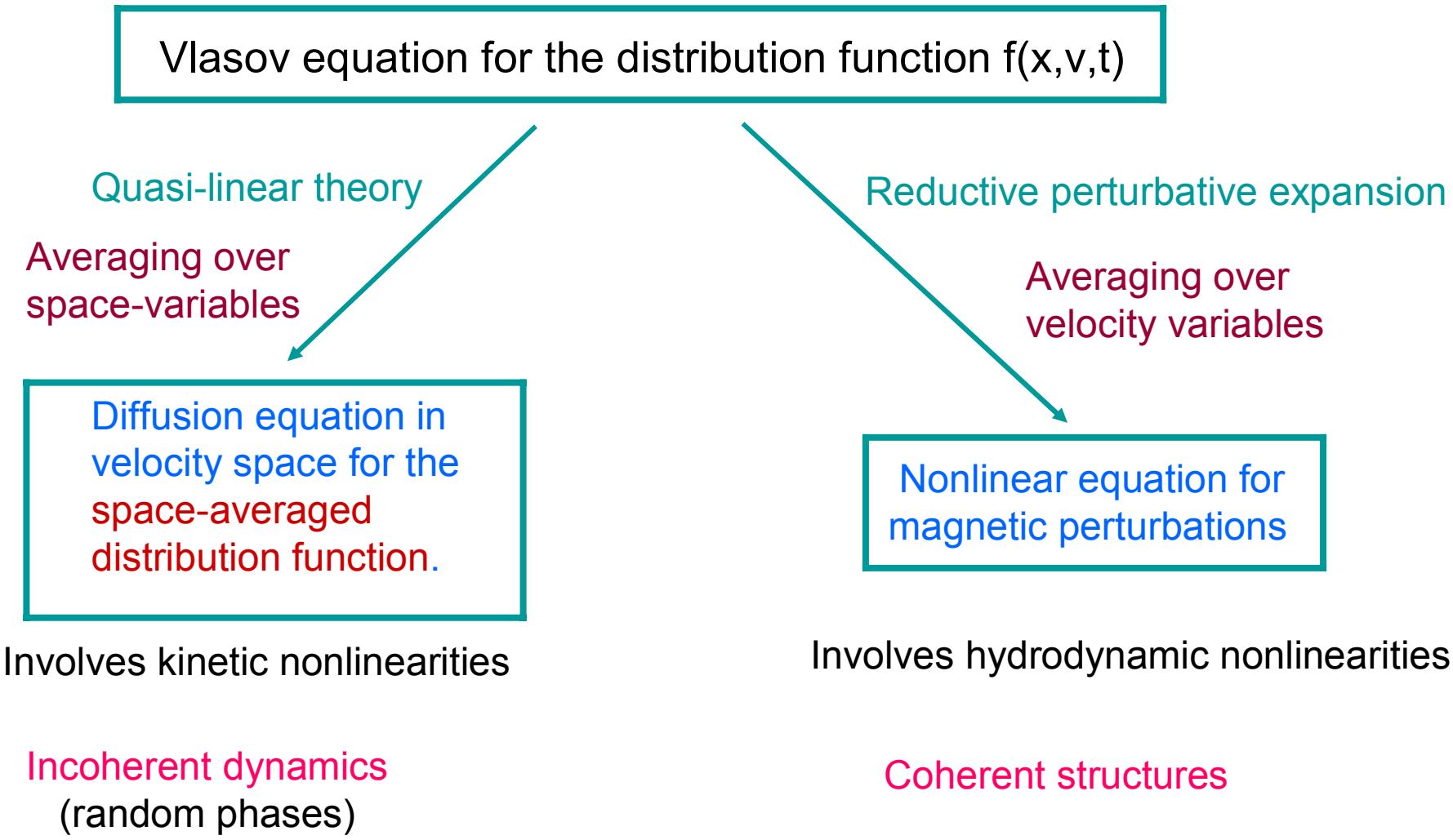
Vlasov equation for the distribution function f(x,v,t)
Quasi-linear theory
Averaging over space-variables
Reductive perturbative expansion
Averaging over velocity variables
Diffusion equation in velocity space for the space-averaged distribution function.
Nonlinear equation for magnetic perturbations
Involves kinetic nonlinearities
Involves hydrodynamic nonlinearities
Incoherent dynamics
(random phases)
Coherent structures

3. Theoretical interpretation

Close to threshold, the linearly unstable mirror modes are confined to large scales.

As structures start to form, it is thus appropriate to study the nonlinear evolution using a reductive perturbative expansion that focuses on the dynamics of the mirror modes.
*(Kuznetsov, Passot and Sulem, PRL, **98,** 235003 ,2007).*

At large scales, kinetic effects (Landau damping and finite Larmor radius corrections) are expected to be weak and to contribute only linearly in the weakly nonlinear regime supposed to develop near threshold.

This argument is validated by a reductive perturbative analysis consistently performed on the Vlasov-Maxwell system.

For the sake of simplicity, assume cold electrons with negligible inertia.

Equation governing the proton velocity (derived from Vlasov equation)

$$\frac{du_p}{dt} + \frac{1}{\rho_p}\nabla \cdot \mathbf{p}_p - \frac{e}{m_p}(E + \frac{1}{c}u_p \times B) = 0$$

Assuming cold electron with no inertia:

$$E = -\frac{1}{c}\left(u_p - \frac{j}{ne}\right) \times B \qquad \text{with} \qquad j = (c/4\pi)\nabla \times B$$

$$\mathbf{p}_p = p_\perp \mathbf{n} + p_\parallel \boldsymbol{\tau} + \boldsymbol{\Pi} \qquad \text{with} \qquad \mathbf{n} = \mathbf{I} - \hat{b} \otimes \hat{b} \qquad \boldsymbol{\tau} = \hat{b} \otimes \hat{b} \qquad \hat{b} = B/|B|$$

$$\rho \frac{du_p}{dt} = \nabla\left(p_\perp + \frac{|B|^2}{8\pi}\right) + \left(1 + \frac{4\pi}{|B|^2}(p_\perp - p_\parallel)\right)\frac{(B \cdot \nabla)B}{\rho_L 4\pi} - \hat{b}\frac{|B|^2}{4\pi}(\hat{b} \cdot \nabla)\left(1 + \frac{4\pi}{|B|^2}(p_\perp - p_\parallel)\right) + \nabla \cdot \boldsymbol{\Pi}$$

In order to address the asymptotic regime, we rescale the independent variables in the form $X = \sqrt{\varepsilon}x$, $Y = \sqrt{\varepsilon}y$, $Z = \varepsilon z$, $T = \varepsilon^2 t$, where ε measures the distance to threshold, and expand any field φ in the form

$$\varphi = \sum_{n=0} \varepsilon^{n/2} \varphi_{n/2}$$

Scaling on space and time variables suggested by the large-scale instability growth rate (ρ_L : ion Larmor radius)

$$\gamma = |k_z| v_{\text{th}\parallel} \frac{\beta_\parallel}{\sqrt{\pi}\beta_\perp}\left[\frac{\beta_\perp}{\beta_\parallel} - 1 - \frac{1}{\beta_\perp} - \frac{k_z^2}{k_\perp^2 \beta_\perp}\left(1 + \frac{\beta_\perp - \beta_\parallel}{2}\right) - \frac{3}{4\beta_\perp}k_\perp^2 \rho_L^2\right]$$

In particular $B_\perp = \varepsilon^{3/2} B_\perp^{(3/2)} + \varepsilon^{5/2} B_\perp^{(5/2)} + \cdots$

$B_z = B_0 + \varepsilon B_z^{(1)} + \varepsilon^2 B_z^{(2)} + \cdots .$

E.B =0
cold electrons
without inertia

$E_\perp = \varepsilon^{5/2} E_\perp^{(5/2)} + \varepsilon^{7/2} E_\perp^{(7/2)} + \cdots$

$E_z = \varepsilon^5 E_z^{(5)} + \varepsilon^7 E_z^{(7)} \cdots .$

One shows that $\nabla_\perp \times B_\perp^{(3/2)} = 0$. By the divergenceless condition : $B_\perp^{(3/2)} = (-\Delta_\perp)^{-1} \nabla_\perp \partial_Z B_z^{(1)}.$

Defining $b_Z = B_Z^{(1)} + \varepsilon B_Z^{(2)}$ and $\overline{p}_\perp = p_\perp^{(1)} + \varepsilon p_\perp^{(2)}$,

the ion-velocity equation reduces to a pressure balance equation

$$\nabla\left[\overline{p}_\perp + \frac{B_0}{4\pi} b_z + \epsilon \frac{b_z^2}{8\pi} + \frac{2}{\beta_\perp}\left(1 + \frac{\beta_\perp - \beta_\parallel}{2}\right) p_\perp^{(0)} (\Delta_\perp)^{-1} \partial_{ZZ} b_z\right] + \epsilon \left(\nabla \cdot \Pi\right)_\perp^{(5/2)} = O(\varepsilon^2)$$

The perpendicular pressure and the gyroviscous force are to be calculated from Vlasov equation

$$\overline{p}_\perp = \beta_\perp \left(1 - \frac{\beta_\perp}{\beta_\parallel}\right) \frac{B_0 b_z}{4\pi} + \varepsilon \frac{\sqrt{\pi}}{v_{th\,\parallel}} \partial_T \left(- \mathcal{H}\, \partial_Z \right)^{-1} \frac{\beta_\perp^2}{\beta_\parallel} \frac{B_0 b_z}{4\pi}$$
$$- \epsilon p_\perp^{(0)} \left[\frac{9}{4\beta_\perp} r_L^2 \Delta_\perp \frac{b_z}{B_0} + \left(1 - 4\frac{p_\perp}{p_\parallel} + 3\left(\frac{\beta_\perp}{\beta_\parallel}\right)^2 \left(\frac{b_z}{B_0}\right)^2\right] \right]$$

$$\left(\nabla \cdot \Pi\right)_\perp^{(5/2)} = -\frac{3}{4}\left(1 - \frac{\beta_\perp}{\beta_\parallel}\right) p_\perp^{(0)} r_L^2 \Delta_\perp \nabla_\perp \left(\frac{b_Z}{B_0}\right)$$

In this near-threshold asymptotics,
- time derivative originates from Landau damping
- Landau damping and finite Larmor radius effects arise only linearly

r_L: ion Larmor radius

After substitution, the leading order cancels out.

Dynamical equation:

$$\partial_T\left(\frac{b_z}{B_0}\right) = \frac{v_{th\parallel}}{\sqrt{\pi}}\frac{\beta_\parallel}{\beta_\perp}\left(-\mathcal{H}\partial_Z\right)\left\{\frac{1}{\varepsilon}\left(\frac{\beta_\perp}{\beta_\parallel}-1-\frac{1}{\beta_\perp}\right)\left(\frac{b_z}{B_0}\right)+\frac{3}{4\beta_\perp}r_L^2\Delta_\perp\left(\frac{b_z}{B_0}\right)\right.$$
$$\left.-\frac{1}{\beta_\perp}\left(1+\frac{\beta_\perp-\beta_\parallel}{2}\right)\left(\Delta_\perp\right)^{-1}\partial_{ZZ}\left(\frac{b_z}{B_0}\right)-\frac{3}{2}\left(\frac{1+\beta_\perp}{\beta_\perp^2}\right)\left(\frac{b_z}{B_0}\right)^2\right\} = O(\epsilon).$$

After simple rescaling

$$\partial_\tau U = \left(-\mathcal{H}\partial_\xi\right)\left[\sigma U + \Delta_\perp U - \Delta_\perp^{-1}\partial_{\xi\xi}U - 3U^2\right]$$

Here, $\sigma = \pm 1$, depending on the positive or negative sign of the threshold parameter $\beta_\perp/\beta_\parallel - 1 - 1/\beta_\perp$.

When the spatial variation are limited to a direction making a fixed angle with the ambient field

$$\partial_T U = \widehat{K}_\Xi\left[\left(\sigma + \partial_{\Xi\Xi}\right)U - 3U^2\right]$$

$\hat{K}_Z = -\mathcal{H}\,\partial_Z$
whose Fourier transform is $|K_Z|$

where Ξ is the coordinate along the direction of variation.

Finite time blowup of the solution

When spatial variations limited to a direction making a fixed angle with the propagation:

$$\frac{\partial U}{\partial T} = \widehat{K}_{\Xi}\left[\left(\sigma + \frac{\partial^2}{\partial \Xi^2}\right) U - 3U^2\right]$$

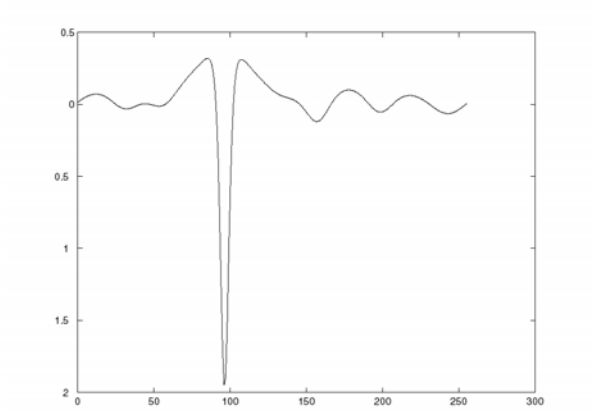

Solution profile near collapse

Integration above threshold (σ>1), with as initial conditions a sine function involving several wavelengths.

After an initial phase of linear instability, formation of magnetic holes, whose number is progressively reduced to one.

After a while, solution blows up with a self-similar behavior.

Wave-particle resonance provides the trigger mechanism leading to the linear instability.

Hydrodynamic nonlinearities reinforce the Instability, leading to collapse.

Linear FLR effects arrest the linear instability at small scales but cannot cope with hydrodynamic nonlinearities.

At the level of Vlasov-Maxwell eqs, the singularity is the signature of the formation of finite-amplitude structures, through a subcritical bifurcation that cannot be captured perturbatively.

Kuznetsov, Passot , Sulem, PRL **98**, 235003, 2007.

The asymptotic equation cannot capture the saturation of the mirror instability.
The asymptotic scaling are broken rather early.

Phenomenological modeling of the saturaturation

Previous models for mirror structures:

(Pantellini et al. Adv. Space Res. **15**, 341,1995, Kivelson and Southwood JGR **101,** 17365 1996, Pantellini JGR **103**, 4789, 1998):

Based on a separation of the particle distribution into trapped and untrapped components that respond differently to magnetic field variations.
Saturation based on the cooling of trapped particles in magnetic troughs.

Usually predict deep magnetic holes and are hardly consistent with the presence of magnetic humps (that are predicted only for exceptionally high values of β)

Bi-stability not addressed.

These models are aimed to describe microscopic processes associated with the existence of coherent structures, rather than the dynamical process leading to their formation.

A saturation mechanism based on the **variation of the local ion Larmor radius** can be phenomenologically supplemented to the asymptotic model, making it consistent with Vlasov-Maxwell simulations.

Motivation:

In regions of weaker magnetic field (and/or large $T_\perp$), ion Larmor radius is larger, making stabilizing effects of finite radius corrections more efficient than in the linear regime. Consequently, mirror instability is more easily quenched in magnetic field minima than in maxima, making magnetic humps more likely to form in the saturating phase of the mirror instability.

$$\partial_\tau U = (-\mathcal{H}\partial_\xi)\left[\sigma U + \Delta_\perp U - \Delta_\perp^{-1}\partial_{\xi\xi} U - 3U^2\right]$$

$$\Delta_\perp U \to \frac{1}{1+\alpha U}\Delta_\perp U + \frac{4}{9}\frac{\nu}{(1+\alpha U)^2}\Delta_\perp^2 U$$

Using conservation of magnetic moment,

$$\rho_L^2 \propto T_\perp/|B|^2 \propto 1/|B| \approx 1/B_z$$

Furthermore, in addition to Laplacian which results from the leading order expansion of a nonlocal operator associated with FLR corrections, we also retain the next order contribution.

ν (taken equal to 0.01) is related to the size of the box

$$\alpha = \frac{2\beta_\perp}{1+\beta_\perp}\left[\beta_\perp\left(\frac{T_\perp}{T_\parallel} - 1\right) - 1\right]$$

Singularity is arrested

Evolution after saturation of linear instability

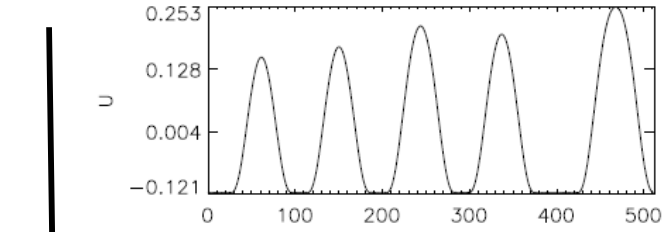

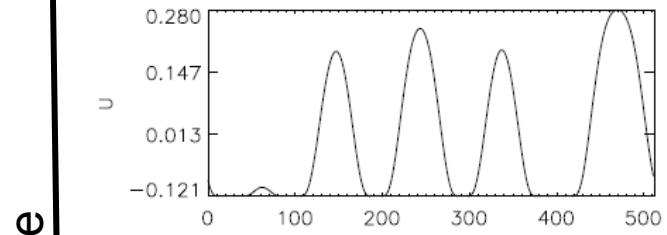

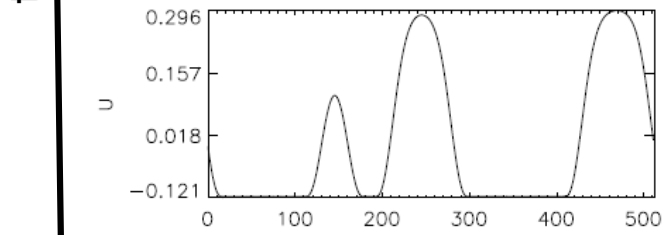

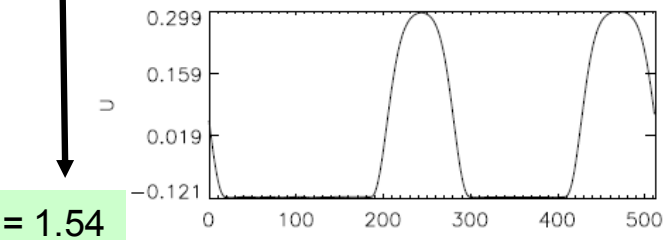

time

$\sigma\alpha$ = 1.54

Coarsening of magnetic humps resulting from the mirror instability in the framework of the phenomenological model.

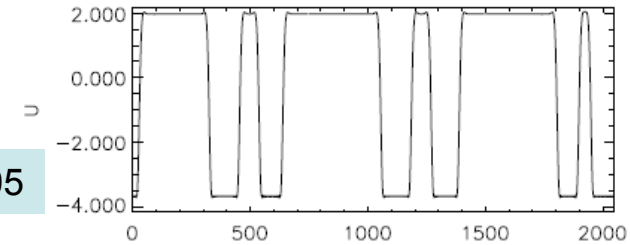

$\sigma\alpha$ = 0.05

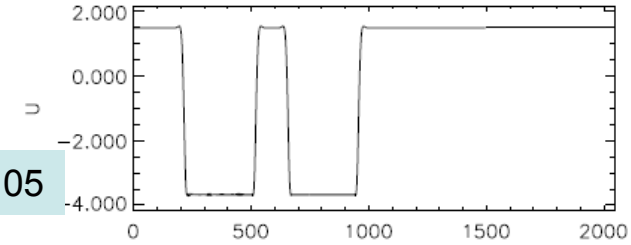

$\sigma\alpha$ = - 0.05

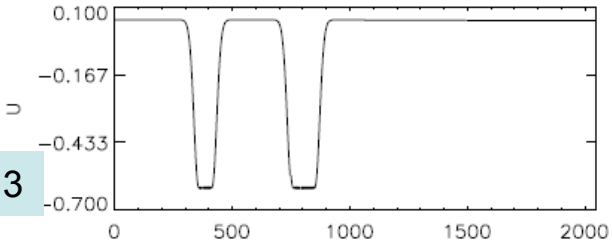

$\sigma\alpha$ = - 0.3

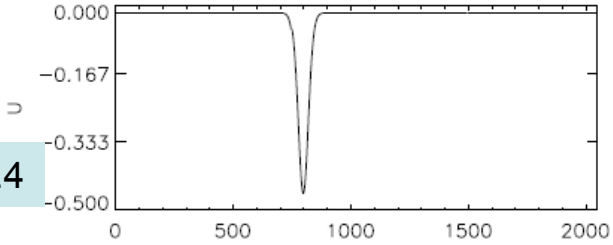

$\sigma\alpha$ = - 0.4

Magnetic holes predicted by the phenomenological model initiated random noise of small amplitude when σ> +1 and large amplitude when σ< -1.

Skewness of magnetic fluctuations
in the quasi-stationary regime

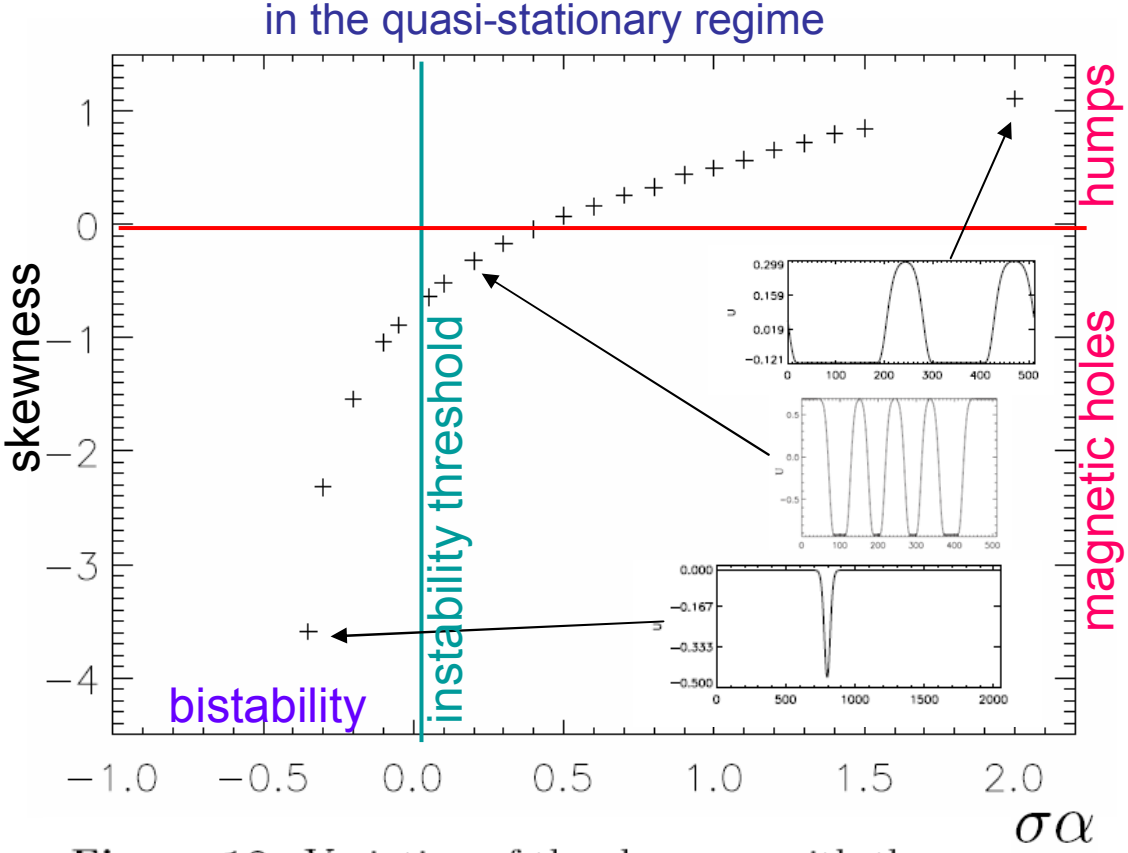

Figure 10. Variation of the skewness with the parameter $\sigma\alpha$, as predicted by the phenomenological model.

I.C.: small-amplitude random noise in supercritical regime
large-amplitude random noise in subcritical regime

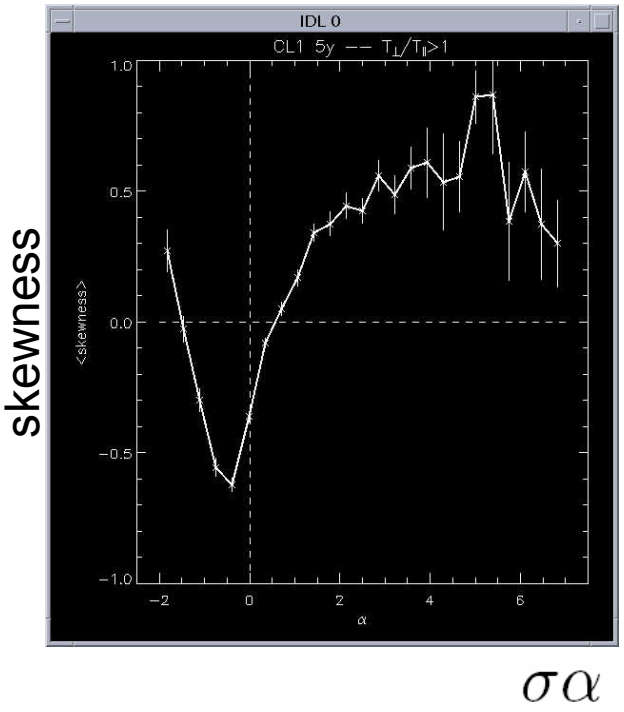

Cluster data : statistic of structures observed in the magnetosheath (courtesy of V. Génot).

4. Formation of magnetic holes

Subcritical solutions (large initial perturbations)

Model simulations

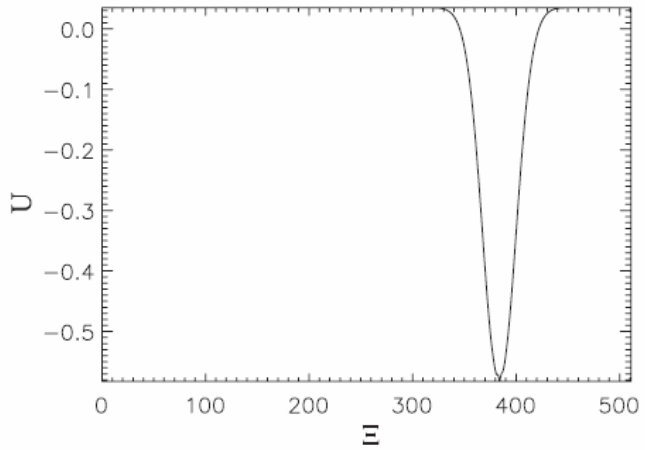

FIG. 4. Quasistatic solution of the saturated equation for $\sigma = -1$, $\nu = 0.01$, and $\alpha = 0.32$, obtained with large initial perturbations.

Vlasov simulation in a small domain

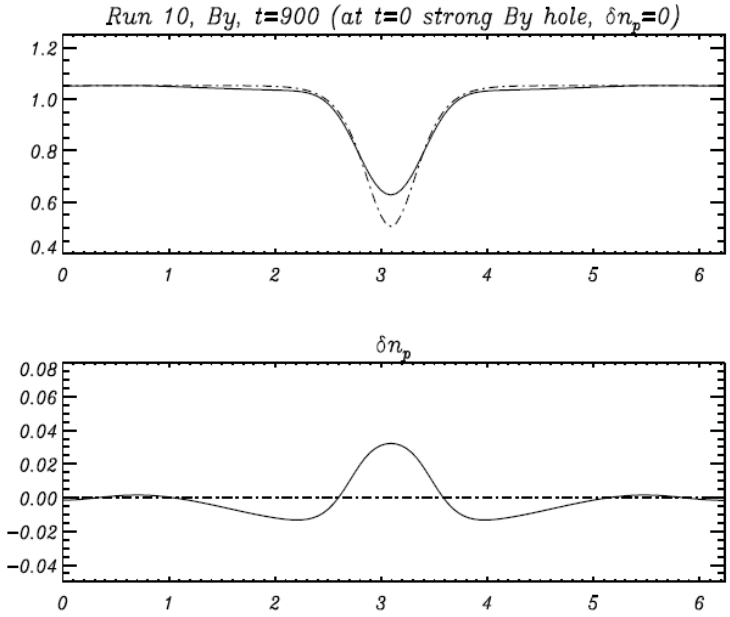

$$\beta_{\|} = 6, \quad \theta = 1.463, \quad T_{\perp} = T_{\|}$$

Large-amplitude magnetic holes survive even far below threshold.

Magnetic humps do not survive

Vlasov simulations in a small domain for **large-amplitude initial perturbations**

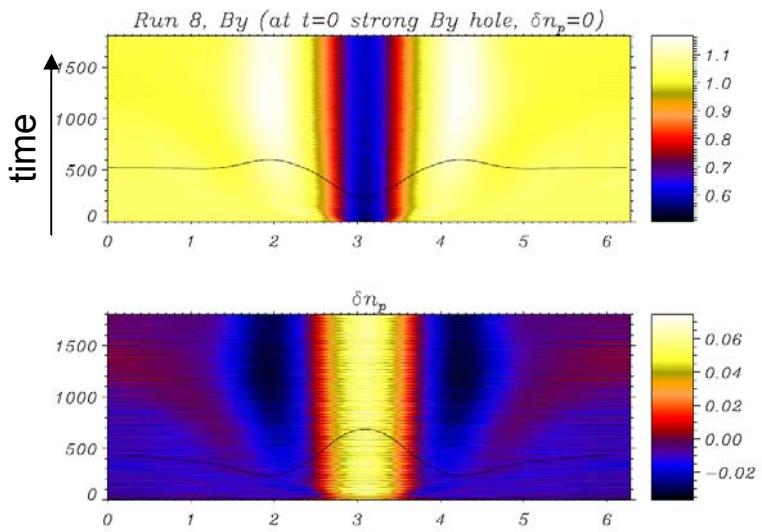

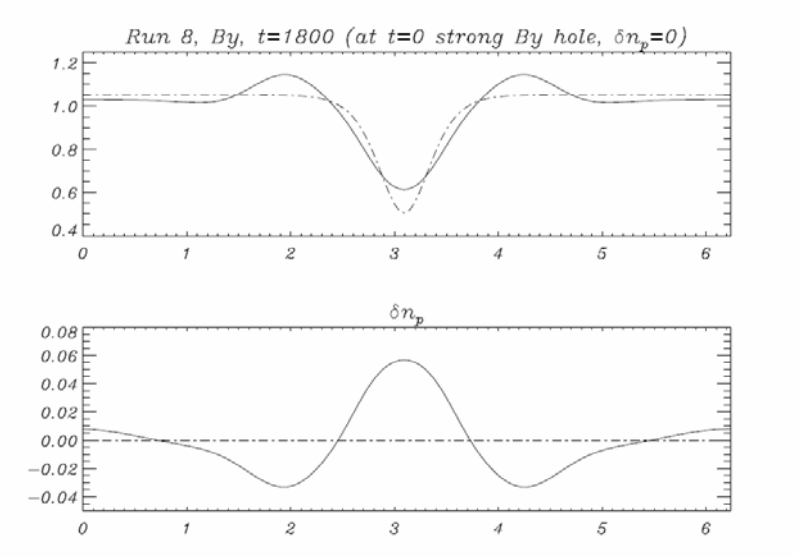

Magnetic hole (and density hump), starting with a large amplitude magnetic field depression, above threshold.

Note the overshoot

Domain size: 15x $2\pi\ c/\omega_{pi}$, with $\beta_{\|}=6$, $T_{\perp}/T_{\|}=1.2$ and $\theta=1.463$

*Magnetic field component perpendicular to the plane (**k, B**o) is symmetric with respect to the center of the magnetic hole: Contrast with soliton models based on anisotropic Hall-MHD (Stasiewiicz 2004, Mjölhus 2006).*

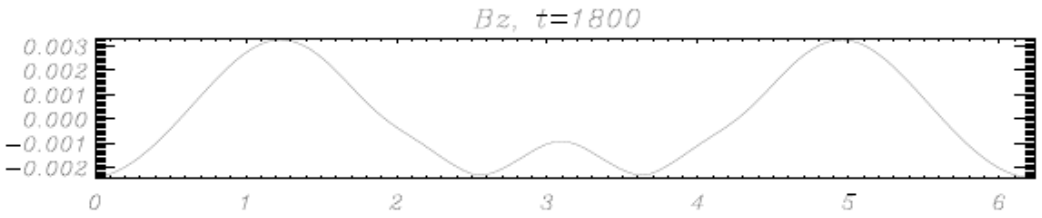

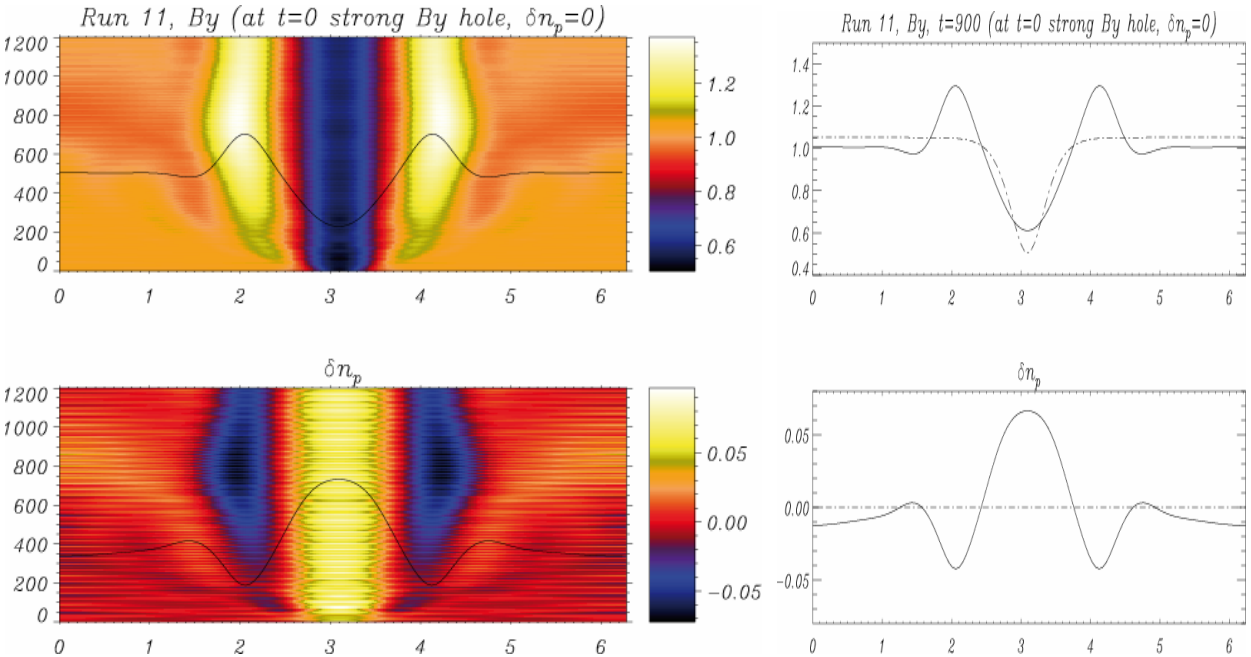

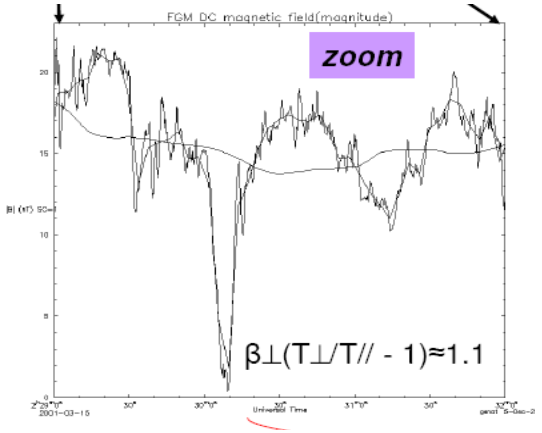

Cluster observation
(Génot et al., AGU 2006)

$$\beta_{\parallel} = 6, \quad \theta = 1.463, \quad T_{\perp}/T_{\parallel} = 1.5$$

Overshoot

With large amplitude initial conditions, magnetic holes are found to be stable solutions even far above threshold.

Formation of **magnetic holes** from small-amplitude noise in a mirror unstable plasma

PIC simulation far from threshold starting form random noise.
At late times, holes form and replace the humps.

1024 cells with 500 000 particles/cell; Domain size=1024 c/ω_{pi}
Growth rate: 0.156 Ω_p^{-1}

$\theta_{kB} = 50.5^o$ (most unstable angle)
$\beta_{p\parallel} = 1 \quad \beta_{p\perp} = 4$
$\beta_e = 10^{-2}$

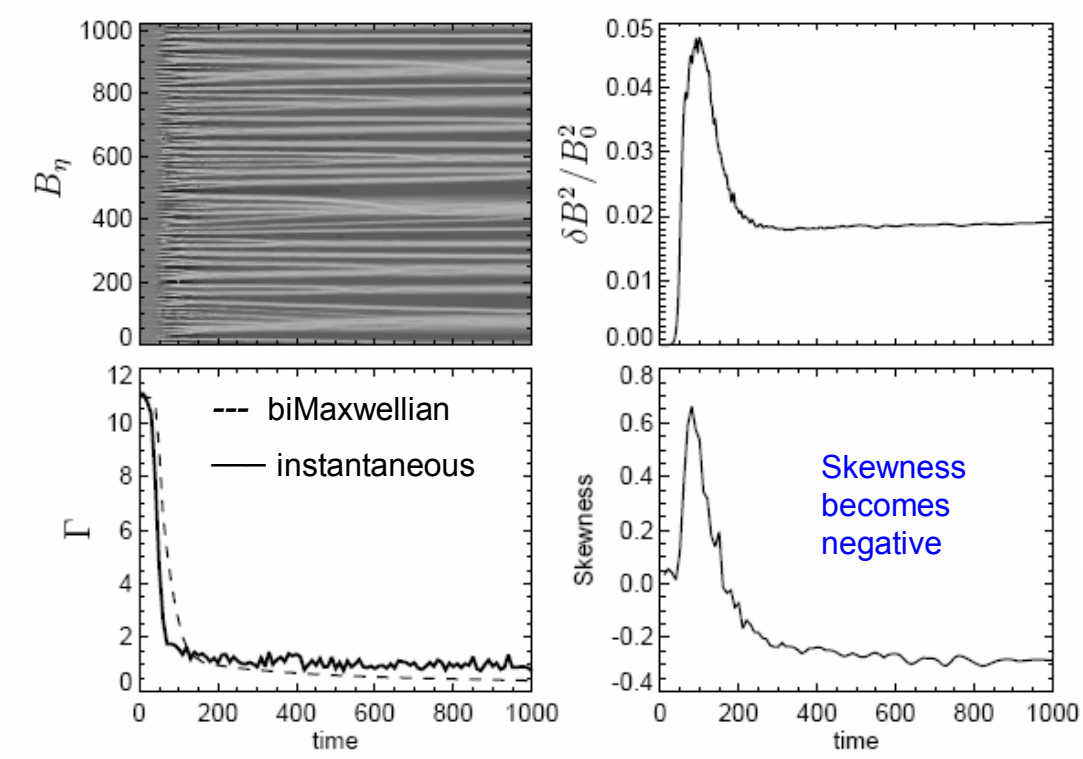

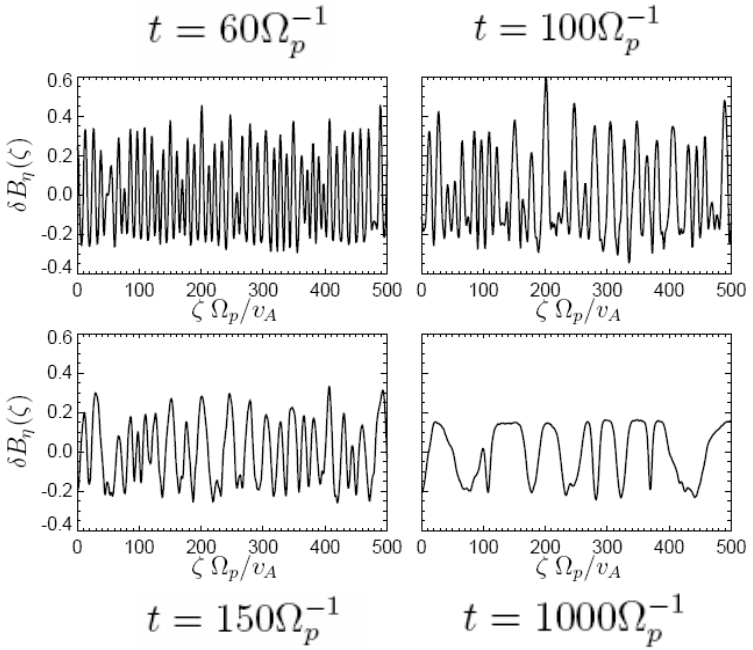

(quarter of the box)

Distance to threshold remains slightly positive.
The system is continuously stirred and coarsening is less efficient.
In particular, there are no isolated structures.

Late transition from magnetic humps to magnetic holes

β is decreasing, which favours nonlinear stability of magnetic holes.

No such transition at larger β (e.g. $\beta_{p\parallel} = 2$).

Resulting magnetic holes:

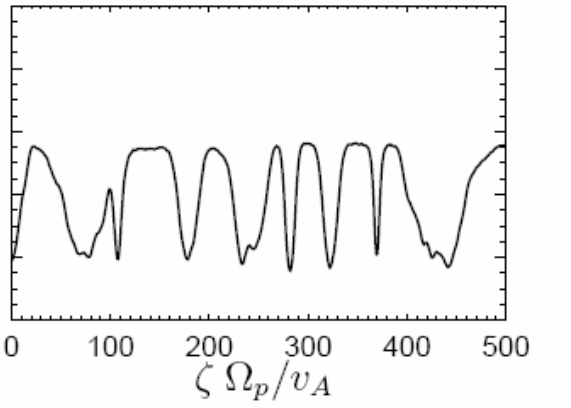

Qualitative similarity with Ulysses measurements in the magnetosheath of Jupiter (Erdös & Balogh 1996):

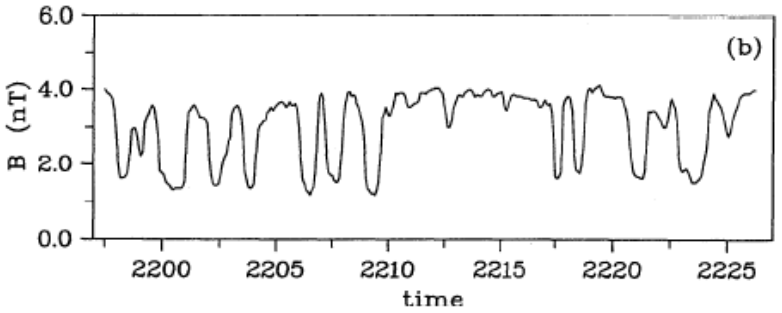

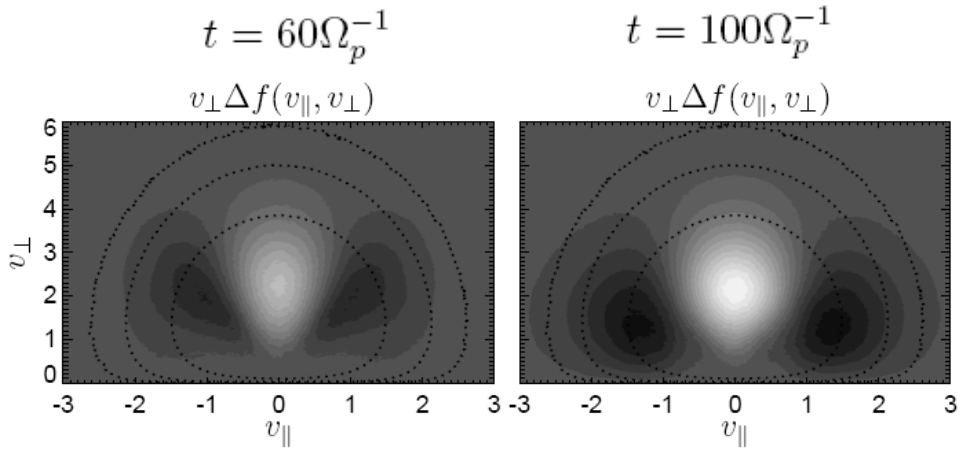

Space-integrated distribution function variation

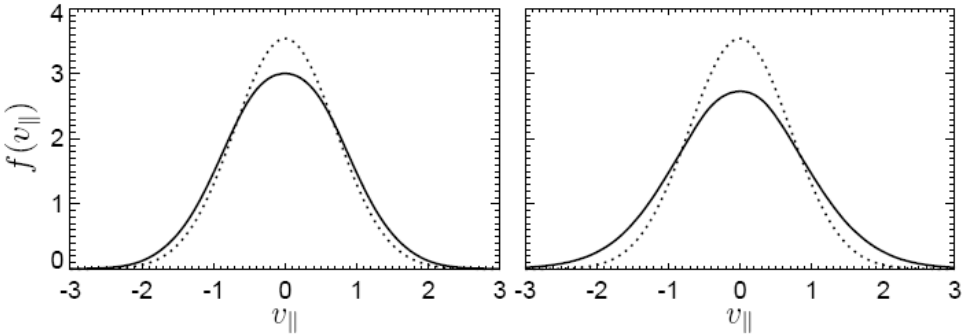

Space-integrated parallel distribution function

The distribution function remains close to bi-Maxwellian.

No flattening of the distribution function.

A scenario for hole formation in the magnetosheath

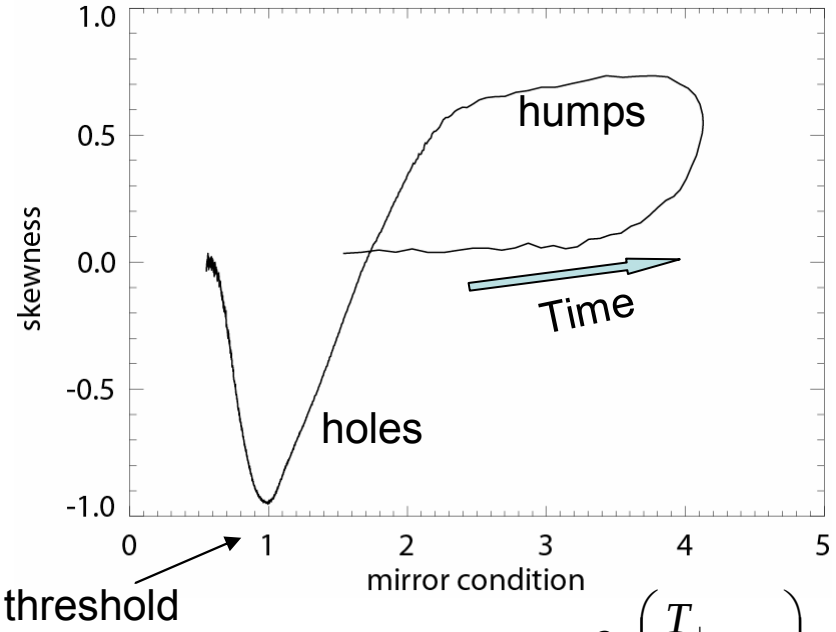

$$R = \beta_{\perp}\left(\frac{T_{\perp}}{T_{//}} - 1\right)$$

Simulations consistent with plasma and mirror mode properties observed by Cluster during magnetosheath path (Sucek, Lucek & Dandouras 2007): magnetic humps evolve into holes as they are convected closer to the magnetosphere within the "plasma depression layer" where the plasma expends and its properties change drastically. In particular, $\beta_{\parallel}$ and R decrease.

PIC simulation in an expanding domain modeling the magnetosheath (Hellinger & Travnicek 2007).

5. Fluid model for mirror modes

(Borgogno, Passot, Sulem, Nonlin. Processes Geophys. **14,** 373, 2007)

Can fluid models describe mirror mode dynamics?

Reproducing linear mirror instability requires
- Landau wave-particle resonance
- (linear) finite Larmor radius (FLR) effects.

It is possible to construct a "FLR Landau fluid"
that generalizes anisotropic MHD by retaining the above effects
(Passot and Sulem, PoP, August 2007).

Extension of Landau fluids (Hammett & Perkins 1990, Snyder et al. 1997), to include transverse scales comparable to the ion Larmor radius, assuming the gyrokinetic scaling.

It consists in **closing the fluid hierarchy** at the level of the 4th order moments, **in a way consistent with the low-frequency linear kinetic theory.**

FLR-Landau fluid retains all hydrodynamic nonlinearities together with LINEAR (or semi-linear) low-frequency kinetic effects.

Linear mirror instability accurately reproduced.

FLR Landau fluid contains all the ingredients of the reductive perturbative asymptotics + additional hydrodynamic nonlinearities that are sufficient to arrest the singularity.

Does not include nonlinear FLR effects: hardly reproduces formation of magnetic humps as the mirror instability saturates.

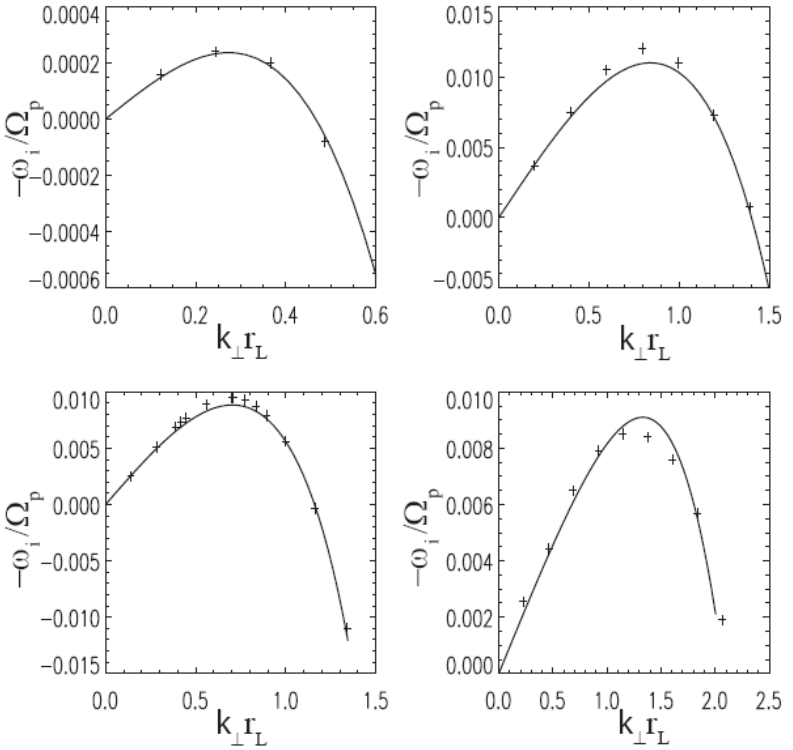

FIG. 10: Normalized growth rate ω_i/Ω_p versus $k_\perp r_L$ for mirror modes with $\beta = 5$, $\tau = 0.1$, $\theta = \cos^{-1}(.1)$, $T_{\perp p}/T_{\|p} = 1.2$ and $T_{\perp e}/T_{\|e} = 1$. (top, left) and $\beta = 2$, $\tau = 1$, $\theta = \cos^{-1}(.1)$, $T_{\perp p}/T_{\|p} = 2$ and $T_{\perp e}/T_{\|e} = 1$. (top, right) as a function of $k_\perp r_L$. Same for $\beta = 5$, $\tau = 1$, $\theta = \cos^{-1}(.2)$, $T_{\perp p}/T_{\|p} = 1.4$ and $T_{\perp e}/T_{\|e} = 1$. (bottom, left) $T_{\perp p}/T_{\|p} = 1.1$ and $T_{\perp e}/T_{\|e} = 1.18$ (bottom, right). $\tau = T_{e\|}/T_{p\|}$

Mirror instability:
Comparison of FLR Landau fluid predictions (crosses) and full linear kinetic theory.

$$T_{//e}/T_{//p} = 0.05, \quad T_{\perp e}/T_{//e} = 1, \quad \cos\theta = 0.2$$

$t = 2000\Omega_p^{-1}$

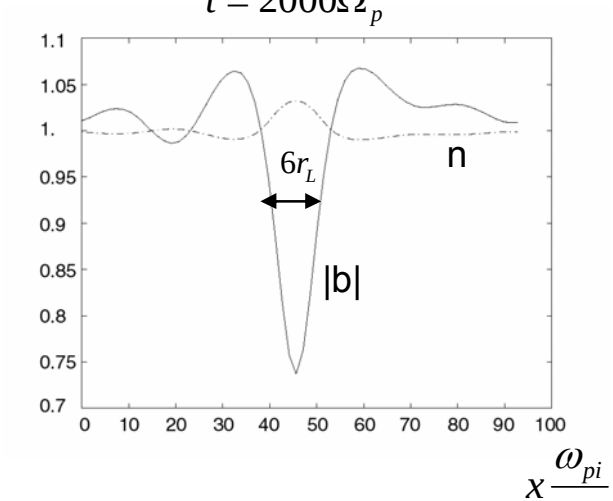

Formation of sharp magnetic holes from initial random noise.

The depth of the hole slowly decreases in time (no effects saturate linear Landau damping)

$t = 850\Omega_p^{-1}$

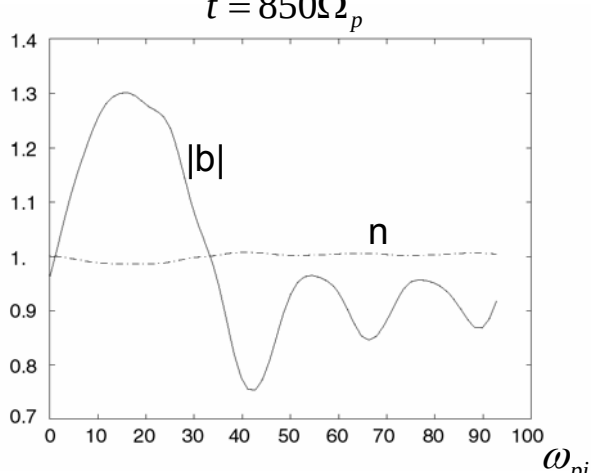

Formation of magnetic humps from initial random noise.

At long times the peak amplitude is observed to decrease and a hole eventually forms.

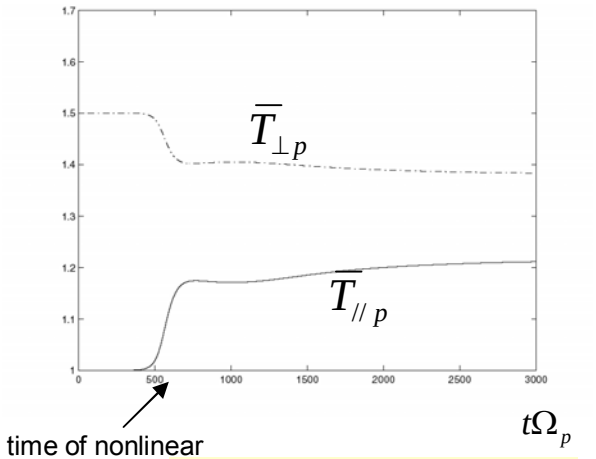

time of nonlinear saturation

$\beta_{// p} = 5, \quad T_{\perp p}/T_{// p} = 1.5$

Mean temperatures

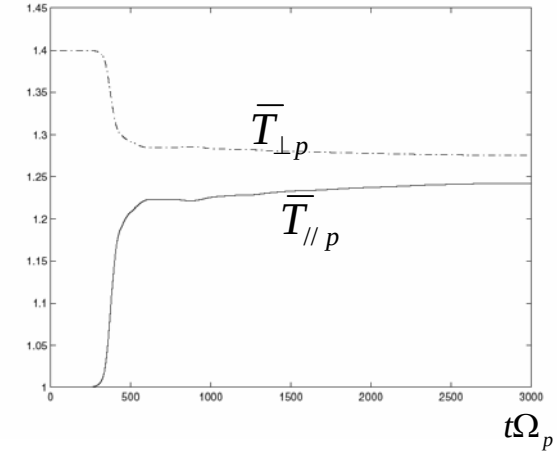

$\beta_{// p} = 20, \quad T_{\perp p}/T_{// p} = 1.4$

During the saturation phase , $\overline{T}_{\perp p}$ and $\overline{T}_{// p}$ evolve in a way that reduces the distance to threshold.

Evidence of bistability

Stationary subcritical magnetic hole solutions
obtained from large amplitude initial conditions,
fixing mean parallel and perpendicular temperatures.

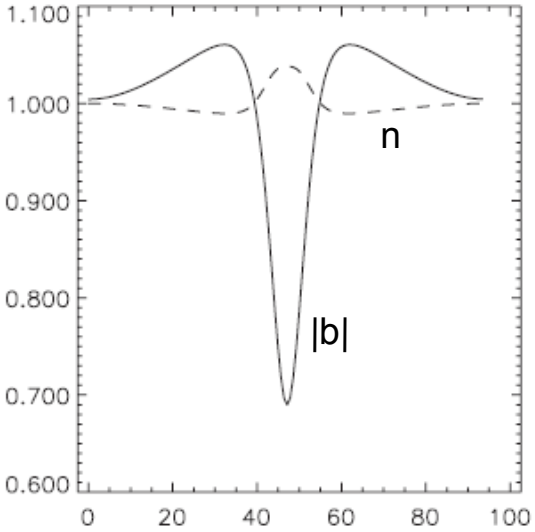

Fig. 6. Magnetic field amplitude (solid line) and density (dashed line) in the stationary regime in a simulation where mean temperatures are kept constant, with $\beta = 5$, $\alpha = 78.46^{\circ}$, $T_{\perp p}/T_{\|p} = 1.17$ and $T_{\perp e} = T_{\|e} = 0.05 T_{\|p}$.

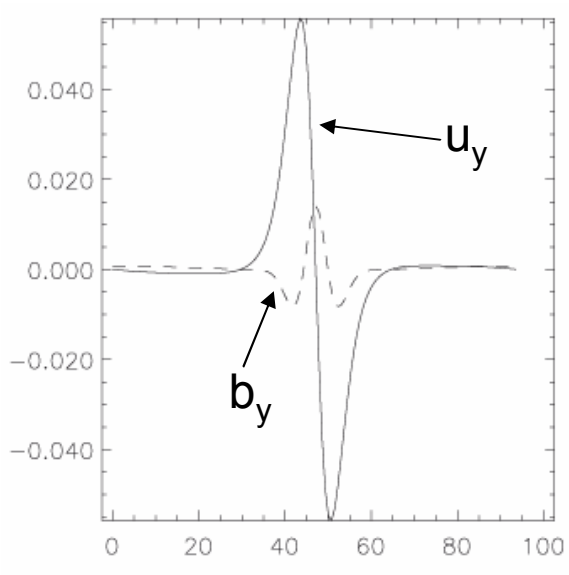

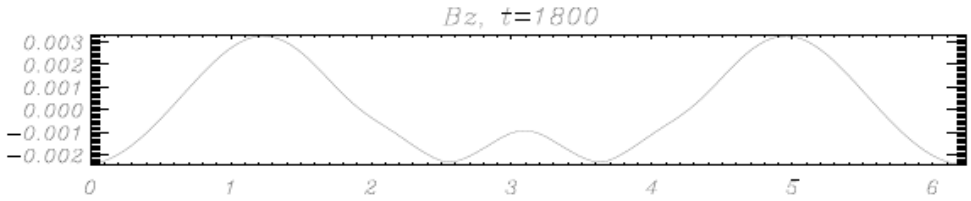

Vlasov simulation

*Magnetic field component perpendicular to the plane (**k**, **B**0) is symmetric with respect to the center of the magnetic hole: Contrast with soliton models based on anisotropic Hall-MHD (Stasiewiicz 2004, Mjölhus 2006).*

Stationarity enforced by maintaining constant the mean proton temperatures
(mimic effect of boundary conditions such as an inflow).

In large domains, formed magnetic patterns are subject to spatio-temporal chaos

$$T_{//e}/T_{//p} = 0.05, \quad T_{\perp e}/T_{//e} = 1$$
$$\beta_{//p} = 2, \quad T_{\perp p}/T_{//p} = 1.43$$
$$\cos\theta = 0.34$$

IC: random noise

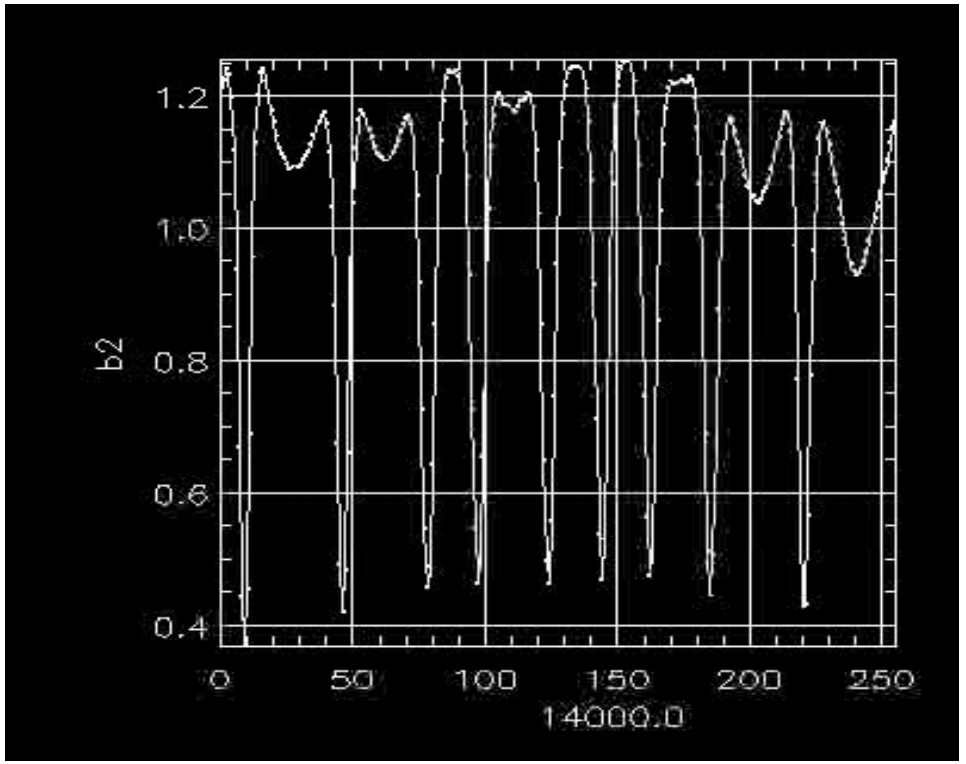

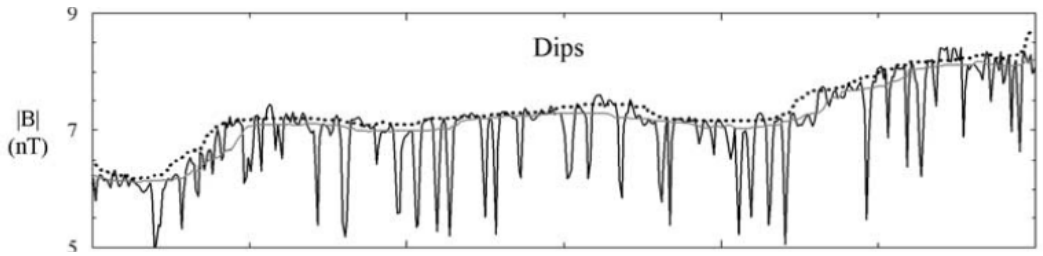

Mirror modes in the Jovian magnetosheath
(Joy et al. 2007)

6. Conclusions

- Numerical integrations of VM equations demonstrate the existence, in large domains, of an early phase described by quasi-linear theory, followed by a regime where coherent structures form.

- In a small domain, no quasi-linear phase is observed.

- The structures resulting from saturation of mirror instabilty are magnetic humps.

- Reductive perturbative expansion performed on the VM eqs near threshold, leads to an equation with a finite-time singularity, signature of a subcritical bifurcation.

- A phenomenological modeling retaining ion Larmor radius variations predicts formation of humps above threshold and holes mainly below threshold (when starting with large amplitude initial conditions), in agreement with CLUSTER observations.

- Numerical integration of VM equation demonstrates the existence of stable holes when initialized with large amplitude fluctuations both above and below threshold.

- Holes can also form in the late evolution of an extended system when initialized far from threshold.
  In this case, β decreases, which makes holes more energetically favored.

- FLR-Landau fluid model can accurately reproduce the linear regime and admits subcritical magnetic hole solutions as well, but hardly leads to magnetic humps.

7. Open questions

- Would it be possible to phenomenologically include effects of local variation of ion Larmor radius in FLR-Landau-fluid?
  Nonlinear FLR are retained by gyrofluids (obtained by closing the moment hierarchy derived from the gyrokinetic equation), but the formalism has not yet developed for anisotropic plasmas.

- Are there conditions (very large domains, very close to threshold) where the instability saturates by quasi-linear effects?

- In a small domain, can one observe, very close to threshold, the signature of the singularity predicted by the reductive perturbative expansion ?

- What is the role of trapped particles?

- How to understand quantitatively the observed transition from humps to holes in large-box simulations far from threshold?

- Is there a unique origin to the commonly observed magnetic holes?

  In particular, are the large-scale (hundreds or thousands ion Larmor radii) magnetic holes observed in the solar wind by Stevens & Kasper (JGR 2007) also associated with the mirror instability?

- What is the role of the mirror structures on the magnetopause boundary?
  Can they trigger micro-reconnection events?